A Pre-Feasibility Assessment of Geologic CO_2 Storage, Offshore Corpus Christi

Jarely Mendez

Thesis submitted to the faculty of the Virginia Polytechnic Institute and State University
in partial fulfillment of the requirements for the degree of

Master of Science
in
Geosciences

Ryan M. Pollyea, Chair
Brian W. Romans
Nino S. Ripepi

May 12, 2025
Blacksburg, Virginia

Keywords: CO_2 storage, carbon sequestration, numerical modeling

A Pre-Feasibility Assessment of Geologic CO_2 Storage, Offshore Corpus Christi

Jarely Mendez

ABSTRACT

Carbon capture and storage (CCS) is a technology to capture CO_2 emissions from industrial point-source facilities and store the CO_2 in deep geological formations in perpetuity. The Gulf of Mexico is a region of interest for CCS development, as it contains laterally extensive reservoir-seal systems comprising Miocene sands with high porosity and permeability that are overlain by low permeability shale. Because the Gulf of Mexico has been greatly characterized for oil and gas exploration, it is a promising region for carbon storage development. Metro areas Corpus Christi and Victoria are known for their refineries, petrochemical, and LNG (liquified natural gas) production, which create emissions along the Texas coast. To identify offshore CO_2 storage within proximity to coastal CO_2 sources, this study assesses the CO_2 storage potential within a set of adjacent leasing blocks in federal waters offshore Corpus Christi. Site characterization is based on a 3D seismic-reflection survey and legacy well-logs to identify regional faults, and an offshore, laterally extensive reservoir and caprock that could be useful for geologic carbon storage. This study develops a geomodel from seismic-reflection data and reservoir properties and then implements numerical simulation to consider four injection scenarios using a single injection. Simulation results storing CO_2 at a rate of 1 MMT/year and 1.7 MMT/year show two potential injection rates that could be safe for storage over a 30-year period. We hope this pre-feasibility study encourages further studies in the offshore Corpus Christi region.

A Pre-Feasibility Assessment of Geologic CO_2 Storage, Offshore Corpus Christi

Jarely Mendez

GENERAL AUDIENCE ABSTRACT

Carbon capture and storage (CCS) is a method to capture CO_2 emissions from industrial point-source facilities and permanently store the CO_2 in deep geological formations. The Gulf of Mexico is a region of interest for CCS development, as porous-permeable sands and low permeability shales are present. Metro areas Corpus Christi and Victoria are known for their refineries, petrochemical, and LNG (liquified natural gas) production, which create emissions along the Texas coast. To identify offshore CO_2 storage within proximity to coastal CO_2 sources, this study assesses the CO_2 storage potential in offshore Corpus Christi federal leasing blocks. Site characterization is based on a 3D geophysical survey and legacy well-logs to identify geological features and properties that could be useful for geologic carbon storage. This study builds a geologic model and then implements computer models for testing four CO_2 injection scenarios assessing the potential CO_2 storage capacity for a single injection well. Simulation results show two potential injection rates that could be safe for storage over a 30-year period. We hope this pre-feasibility study encourages further studies in the offshore Corpus Christi region.

Table of Contents

List of Figures

List of Tables

Introduction

Carbon capture and storage (CCS) is a method in which CO_2 emissions are captured from point sources or the atmosphere and injected into deep geological formations in a supercritical phase to be stored long-term (Bandilla, 2020; Bashir et al., 2024). Although the technology required for CCS has been available for decades, recent policy decisions (taxes, credits, and subsidies) worldwide are now driving widespread adoption of CCS as a technological strategy to reduce greenhouse gas emissions (Ma et al., 2022). As early as the 1960s, the idea of injecting CO_2 into the subsurface originally served the purpose of Enhanced Oil Recovery (EOR), a technique where CO_2 injection helps extract remaining oil from mature fields in several basins across North America. (Godec et al., 2013; Ma et al., 2022; National Energy Technology Laboratory, 2020). More recently, industry-scale projects have focused specifically on long-term geologic CO_2 storage, focusing on capturing and storing CO_2 from large emitters (e.g., electricity production, cement manufacturing, etc.) as a technological strategy to reduce anthropogenic CO_2 emissions, thus taking steps towards climate change mitigation (Bashir et al., 2024; Bump & Hovorka, 2024). Throughout the U.S., many areas produce vast amounts of CO_2 that could benefit from industry-scale geologic storage to reduce their emissions, and ongoing research continues to open new geologic environments for geologic CO_2 storage. For example, CO_2 can be stored in saline formations comprising porous and permeable rocks where pore space is saturated with non-potable brine, un-mineable coal seams, and depleted oil and gas reservoirs (Figure 1*)*. More recently, research suggests that CO_2 can also be stored in fold-and-thrust belts (Koehn, et al., 2023a), large-igneous provinces (Pollyea et al., 2014), and carbonate platforms (Orivri et al., 2025). This study investigates the amounts of CO_2 that could be stored in a saline aquifer in Matagorda Island leasing blocks, offshore Texas.

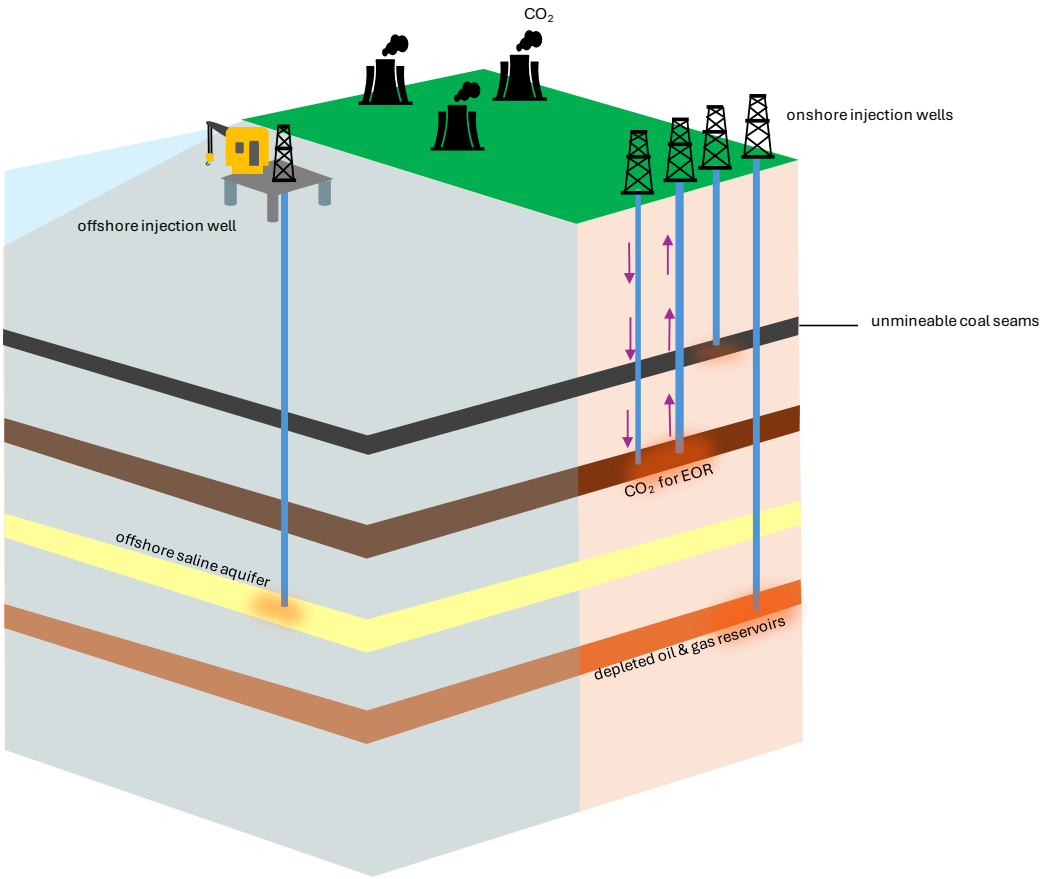

Figure 1. Uses of CO_2 for storage and EOR. Adapted from (Bashir et al., 2024)

Advantages of offshore CO_2 storage

Geologic carbon storage projects can take place onshore and offshore; however, offshore carbon storage is logistically safer and more advantageous as it avoids heavily populated regions, could benefit from existing infrastructure, and only requires dealing with a single landowner, as pore space is owned by government bodies and may simplify leasing rights (Schrag, 2009). U.S. Federal offshore storage estimates show a total storage potential of 490-6,454 billion metric tons of CO_2 and formation fluid offshore has a chemistry and salinity (30,000 to 40,000 ppm total dissolved solids) similar to seawater (National Energy Technology Laboratory, 2015; Schrag, 2009).

Saline formations show potential for dependable and long-term CO_2 storage. Appropriate saline aquifers for CO_2 storage are typically at depths of 800-3,000 meters, contain porous and

permeable sedimentary rocks and are geographically widespread throughout North America (Bashir et al., 2024; National Energy Technology Laboratory, 2015). Saline aquifers generally occur at depths deeper than freshwater, and as offshore basins are entirely saline, there is no risk of contaminating drinking water resources. Offshore saline formations allow for a shallower storage depth below the seabed in comparison to onshore sites due to the water columns increasing the pressure on the formation, thus decreasing the depth at which CO_2 will exist in a supercritical state (7.4 MPa and 31° C). Moreover, in 2008, the U.S. Environmental Protection Agency (EPA) mandated that saline storage have a minimum pore water total dissolved solids (TDS) concentration of at least 10,000 ppm to protect potential potable water supply; this environmental requirement is not likely to be an issue offshore (Craddock et al., 2012). The combination of these geologic and regulatory factors makes offshore basins a promising location for saline aquifer storage. An example of a successful offshore CO_2 storage project is the Sleipner Project located in the North Sea. (Bashir et al., 2024; Chadwick et al., 2004; Ma et al., 2022). Here the Utsira Sand Formation, a saline aquifer, serves as a CO_2 storage reservoir at a depth of ~1,000 meters, where 1 million metric tons of CO_2 are stored per year (Chadwick & Eiken, 2013; Korbøl & Kaddour, 1995; Solomon, 2007). Through this project, over 20 million tons of CO_2 have been stored since 1996 (Ma et al., 2022; National Energy Technology Laboratory, 2015). This project is still operating today and is being monitored through both seismic and gravimetric methods to confirm the secure storage of the CO_2 that was injected (Alnes et al., 2011; Arts et al., 2004; Furre et al., 2017; Singh et al., 2025). The Sleipner Project demonstrates the ability of offshore basins to store millions of tons of CO_2 in saline aquifers (Koehn, et al., 2023b).

Geological Setting: Gulf of Mexico

In the southern United States, the Gulf of Mexico is a highly productive region for offshore oil and gas production. In the fiscal year 2024, offshore federal production reached ~668 million barrels of oil (Bureau of Ocean Energy Management (BOEM), 2025a). The Gulf of Mexico is geologically promising for CO_2 storage as previous data proves the existence of laterally extensive sands of up to hundreds of meters in thickness, porosities of 20-35%, and permeabilities ranging from 10^{-13}-10^{-12} m^2 (100 mD-1 D) (Bureau of Ocean Energy Management (BOEM), 2020). Because there is a vast amount of data available, existing infrastructure, and proximity to concentrated emission sources, the Gulf of Mexico shows high potential for carbon storage development. (Bump & Hovorka, 2024; Koehn, et al., 2023b; Meckel et al., 2021; Sachde et al., 2022).

The Gulf of Mexico is an offshore basin that began forming ~200 million years ago through crustal extension, seafloor spreading, and high sediment supply and accumulation from the North American continent (Galloway, 2008). The Gulf of Mexico depocenter has sediments from the Jurassic through the Holocene, with strata up to twenty kilometers thick. Thick salt, known as the Louann salt, was deposited across most of the basin during the mid-to-late Jurassic period. Mobilization and deformation of the salt due to subsequent sediment loading led to large-scale structures (e.g., stocks and canopies) over much of the basin, which influenced the dispersal and accumulation of sedimentation throughout the Cenozoic (Galloway, 2008). Towards the end of the Mesozoic, thermal subsidence resulted in general basin deepening providing accommodation for sediment deposition. North American sediments filled almost half of the basin since then.

The Gulf of Mexico has been explored for over 100 years for its energy resources (Galloway, 2008). Hydrocarbon deposits are found throughout the basin reservoirs of almost

every depositional period, including the Miocene, Oligocene, Paleocene-Eocene, Plio-Pleistocene, upper Cretaceous, and Jurassic strata. Exploration in this region led to the discovery of oil within Paleogene and Miocene reservoirs beneath the continental slope, and also in sand and shale gas deposits in the Jurassic and early Cretaceous formations (Galloway, 2008). Success in oil and gas in the Gulf of Mexico is possible through its history of high sediment deposition, porous rocks, gravity-induced mass wasting and deformation, and salt migration creating various reservoir and trap types. The geology of the Gulf of Mexico is suitable for carbon storage through its high porosities, high permeabilities, and known seals, which are low permeability formations that can physically trap CO_2 within the target reservoir formation (Sachde et al., 2022; Wallace et al., 2014). In summary, the Gulf of Mexico presents a compelling opportunity for carbon emissions from proximal (i.e., coastal) industrial facilities to be stored offshore from states, like Texas, by repurposing existing data and applying similar concepts from oil and gas projects.

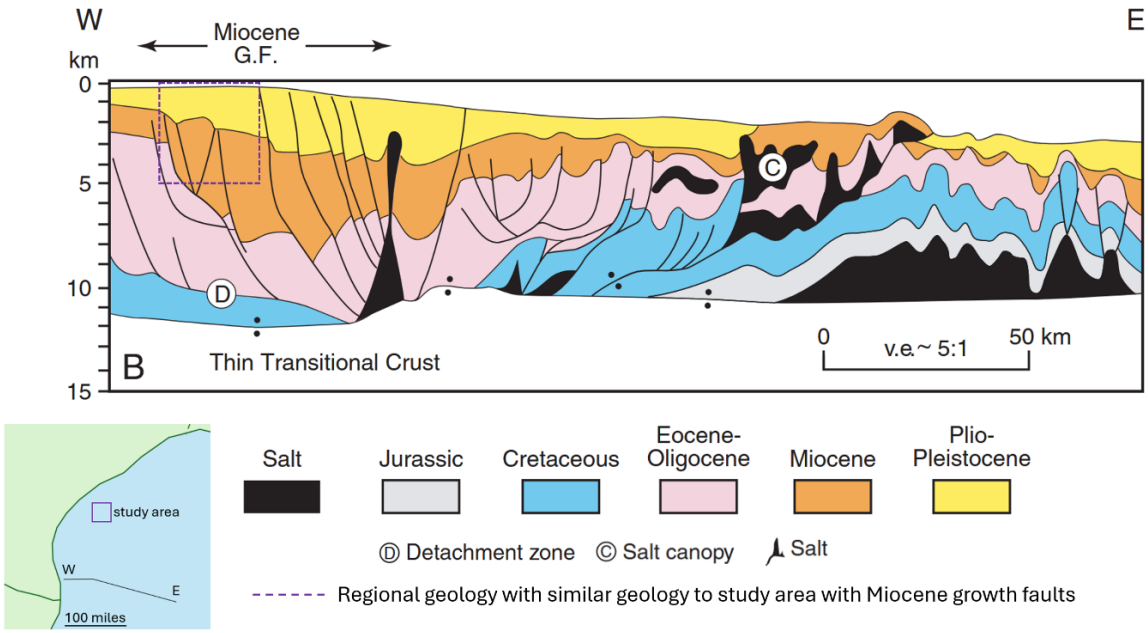

Figure 2. Cross-section of the northwestern Gulf of Mexico continental margins. Adapted from (Galloway, 2008). Dashed purple box (upper left) denotes general geologic setting for the study area in this project.

Offshore Texas Decarbonization and CO_2 storage potential

In Texas, about 82% of greenhouse emissions consist of CO_2 (Texas Commission on Environmental Quality (TECQ), 2024). The state of Texas has high industrial emissions from industries such as power plants, chemicals, refineries, and petroleum & natural gas systems totaling up to over 360 million metric tons (MMT) of CO_2 emissions from over 700 facilities (EPA, 2024). These emissions sources, such as the ones from the industrial metro areas Corpus Christi and Victoria, Texas, are near offshore leasing areas, making them ideal for CO_2 point-source capturing and transportation (Figure 3).

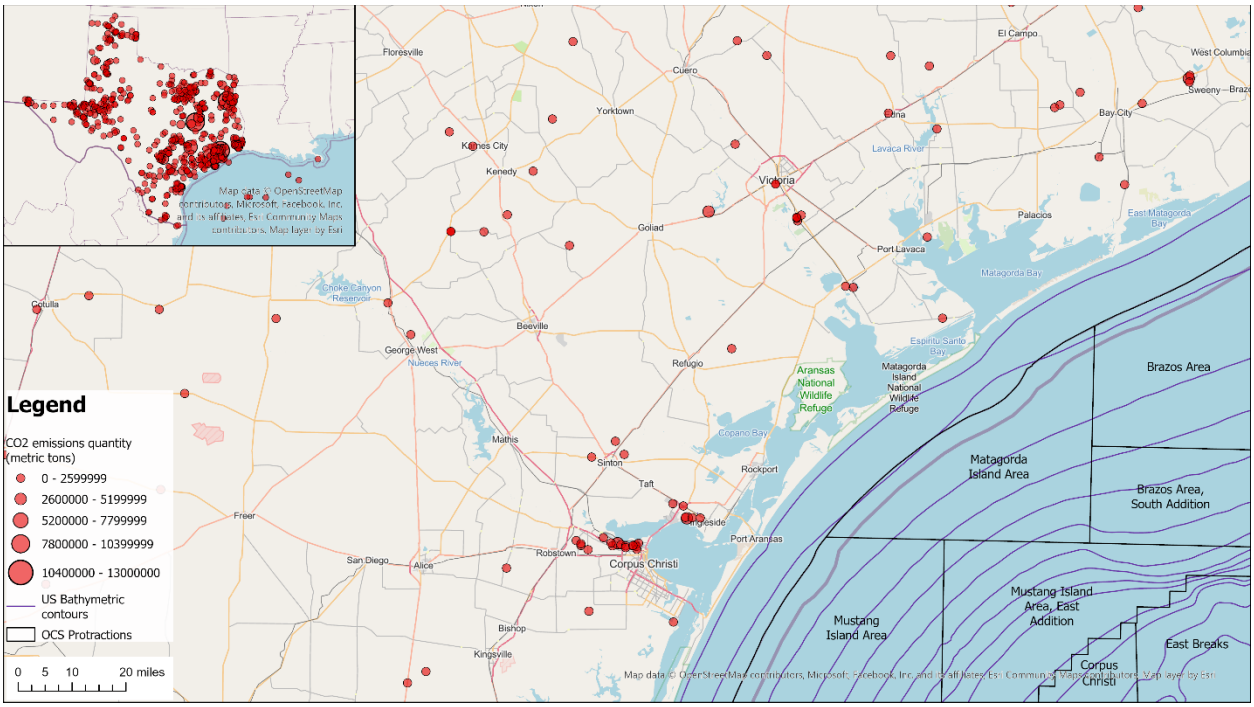

Figure 3. Corpus Christi and Victoria, TX emissions locations to Matagorda Island leasing area. (Bureau of Ocean Energy Management (BOEM), 2025b; EPA, 2024). Specific study area not shown at the request of data provider.

The Texas Continental Shelf could have the appropriate properties for storing this CO_2 offshore. The Texas Continental Shelf consists of rapid deposition of sediments during the Cenozoic and simultaneous growth faulting (Ajiboye & Nagihara, 2012; Foote et al., 1992). Along the Texas shelf, there are multiple growth fault systems subparallel to the shelf margin: the Frio Fault zone, the Clemente-Tomas, the Corsair, and the Wanda fault system (Ajiboye &

Nagihara, 2012; Galloway, 2008). Within the study area for this project, the major Clemente-Tomas and Corsair faults are present, as well as secondary faulting both dipping SE. Minor synthetic faults for the Clemente-Tomas and Corsair faults dip in the same direction and minor antithetic faults are dipping in the opposite direction. The Texas Continental Shelf holds Miocene sands, which are known for oil and gas production, making it a geologic interval of interest for CCS. As decarbonization efforts increase, offshore Texas is being considered by companies for geologic carbon storage hub development (Wallace et al., 2014).

Methods

Geologic Data

Data available includes a 3D seismic-reflection survey in the Matagorda Island leasing area and geophysical logs from 14 legacy wells donated by GeoTomo LLC, including depths and formation tops, and BOEM's Gulf of Mexico Sands Dataset and Biostratigraphic Chart of the Gulf of Mexico offshore region (Bureau of Ocean Energy Management (BOEM), 2020; Witrock, 2017). At the request of GeoTomo, the specific location of the 3D seismic dataset is being withheld from this thesis; however, the general location falls within the coastal region illustrated in Figure 3. The BOEM Sands dataset provides information on oil and gas sands from the Gulf of Mexico, including chronozones, play types determined by depositional facies and sediment/structure type, BOEM field numbers, and properties such as porosity and permeability. This information is used to filter through leasing blocks in the survey that had the most production/recovery, high porosities of >20%, and high permeabilities of >100 mD. Figure 4 and Figure 5 show the probability distribution of porosity and permeability values for Lower Miocene sands at depths of 7,000-9,000 feet.

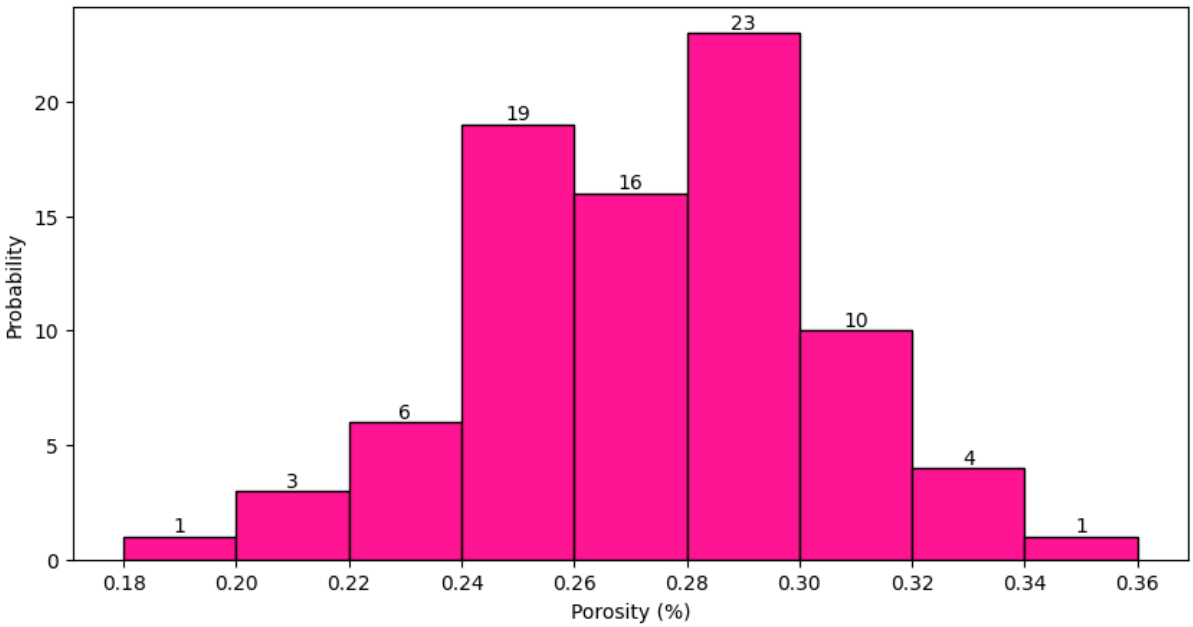

Figure 4. Lower Miocene porosity values at depths of 7,000-9,000 feet. (Bureau of Ocean Energy Management (BOEM), 2020).

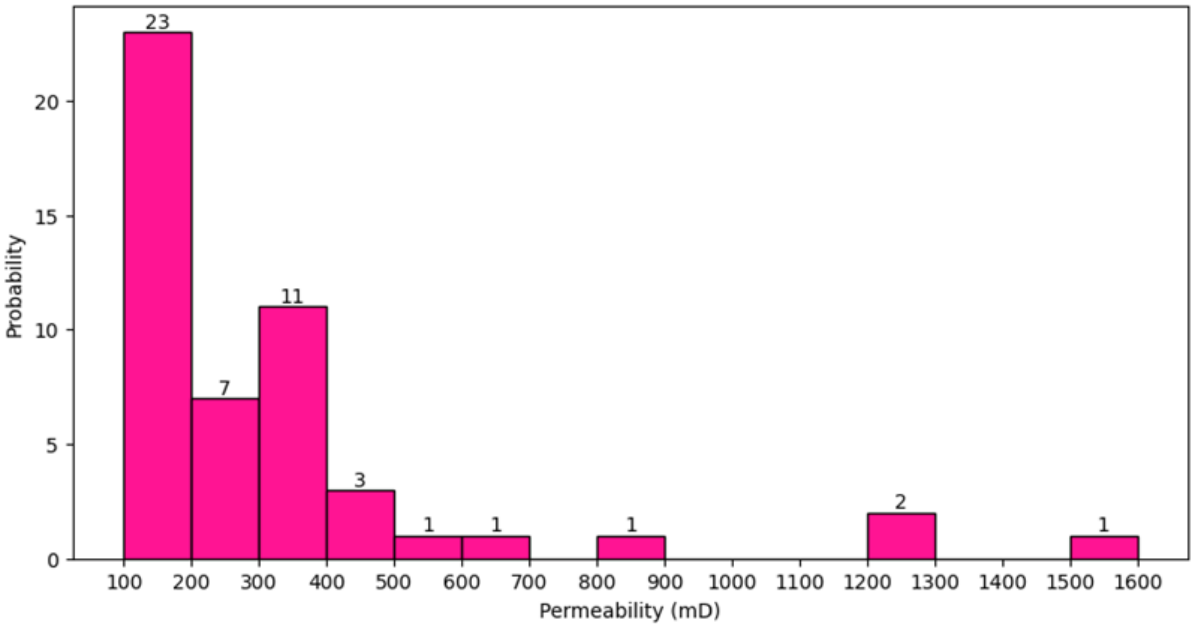

Figure 5. Lower Miocene permeability values at depths of 7,000-9,000 feet. (Bureau of Ocean Energy Management (BOEM), 2020).

Seismic Interpretation

The following criteria are used to determine a potential reservoir: close proximity to shore at federal waters, a low dip region of < 5 degrees, lateral continuity of the reservoir and caprock, and depth ranges allowing CO_2 to be injected in a supercritical phase. The injection well would also need to be away from the Clemente-Tomas fault to prevent the CO_2 from reaching it, and prevent pressure build-up that could induce seismicity (Pollyea et al., 2014).

Laterally extensive seismic-stratigraphic units in the survey area are identified as potential carbon storage zones. This survey area is ~796 square miles, has a time range of 0-7.996 seconds two-way travel time, and holds 1,010 inlines running NE-SW by 825 crosslines running NW-SE. The Clemente-Tomas and Corsair growth faults are mapped across the study region. A seismic time slice at ~1.4 seconds revealed areas of complexity due to minor faulting, and unfaulted areas that are close to shore; criteria used to identify an area of the Matagorda Island leasing area showing potential for carbon storage development. Bio-stratigraphic markers from the available well data and the BOEM Biochart (Witrock, 2017) are identified within the seismic reflection data, revealing the age of the seismic survey ranged from Lower Pliocene to Lower Miocene, and the reservoir of interest is Lower Miocene aged (Figure 6). This includes benthic foraminiferal markers from the middle and lower Miocene: *Bigeneria humblei*, *Amphistegina "B"*, *Robulus "L" / 43*, *Discorbis bolivarensis / "B"*, and *Marginulina ascensionensis / "A"*. These markers are found in well formation top reports and published literature with a similar study area to ours (Ajiboye and Nagihara, 2012). Horizons are mapped for each of the biomarkers, and the reservoir and seal which are identified by log depth and seismic amplitude (impedance contrasting) at a depth suitable for storage. Seismic facies for the area of interest are very continuous, parallel, and have low through high amplitude, but horizon dip increases as it approaches major Clemente-Tomas faulting.

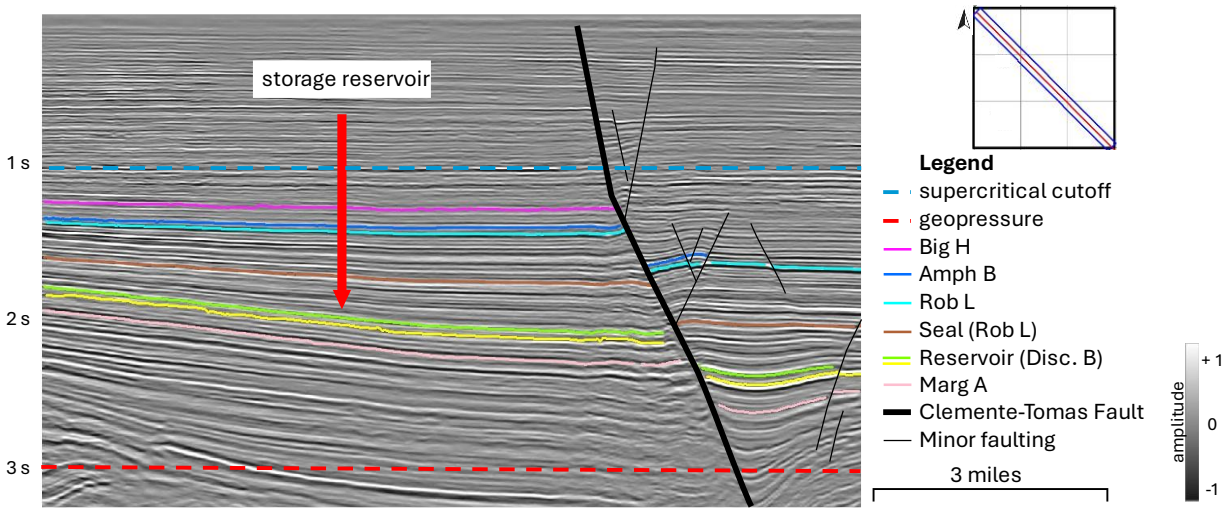

Figure 6. Bio-stratigraphic horizons, seal and reservoir in 3D seismic.

Lower Miocene Depositional History

The Lower Miocene strata in this region compromise offshore shelf deposits that developed as a result of numerous cycles of progradation, flooding, and retrogradation. In the northwestern part of the Gulf of Mexico basin, the Lower Miocene developed from Paleogene sediment supply from northwestern fluvial systems to Neogene sediment from fluvial systems entering the basin from the north (Trevino & Rhatigan, 2017). Its succession was an eight-million-year depositional period with high sedimentation following the Anahuac transgression (Galloway, 2008). Approximately 18 million years ago, another transgression split the Lower Miocene into 2 sequences (Galloway, 2008). A 2 Ma year-long period of retrogradation and transgression ended this period and marked the maximum flooding surface of the *Amphistegina* shale, which is named after the *Amphistegina B* faunal top, and the end of the Lower Miocene (Galloway, 2008).

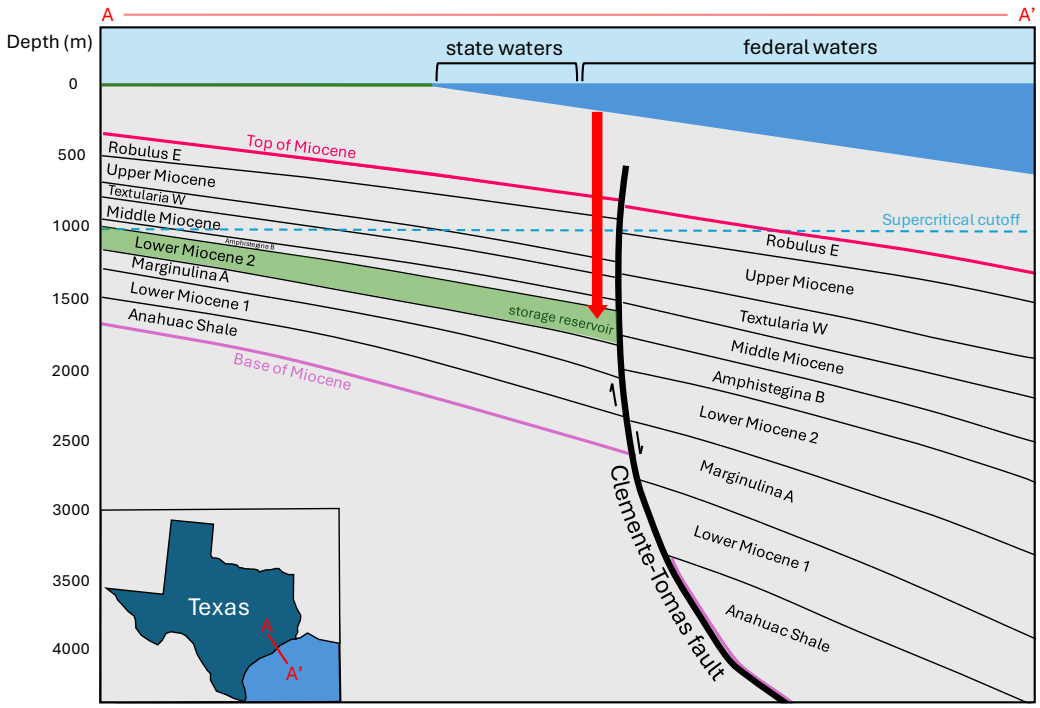

Figure 7. Miocene stratigraphic cross section. Red arrow denotes proposed injection. Adapted from (Wallace et al., 2014)

Well-logs

Key logs used in conjunction with the seismic include spontaneous potential (SP) logs measuring the electric potential variations to identify permeable formations, resistivity (RES) logs to distinguish between hydrocarbons or water-filled formations, bulk density (RHOB) measuring formation density to determine porosity, and neutron porosity (NPHI) logs estimating porosity through amounts of hydrogen from fluids in the pores. SP helped identify saline aquifers where the log deflects towards the left; Low resistivity identified saline aquifers; NPHI and RHOB logs are combined to distinguish between sand or mud dominated layers. Scales for each log are -50 through 80 mV for SP to, 0-4 ohms for resistivity, 1.95-2.95 G/CC for density, and 20-50% for neutron porosity (Figure 8). Seismic-well ties helped identify a caprock for CO_2 containment at ~7,100 ft depth, saline aquifers that could serve as a reservoir at ~7,900 ft depth, and geopressure depth at ~9,000 ft. Formation tops were correlated through logs from 7 legacy wells in the area of interest. These tops were then used to convert the seismic TWT data to depth

in feet using the Dynamic Depth Conversion tool, by providing mapped horizons in time, correlated formation tops in depth identified through the logs, and a fault polygon for the Clemente-Tomas fault.

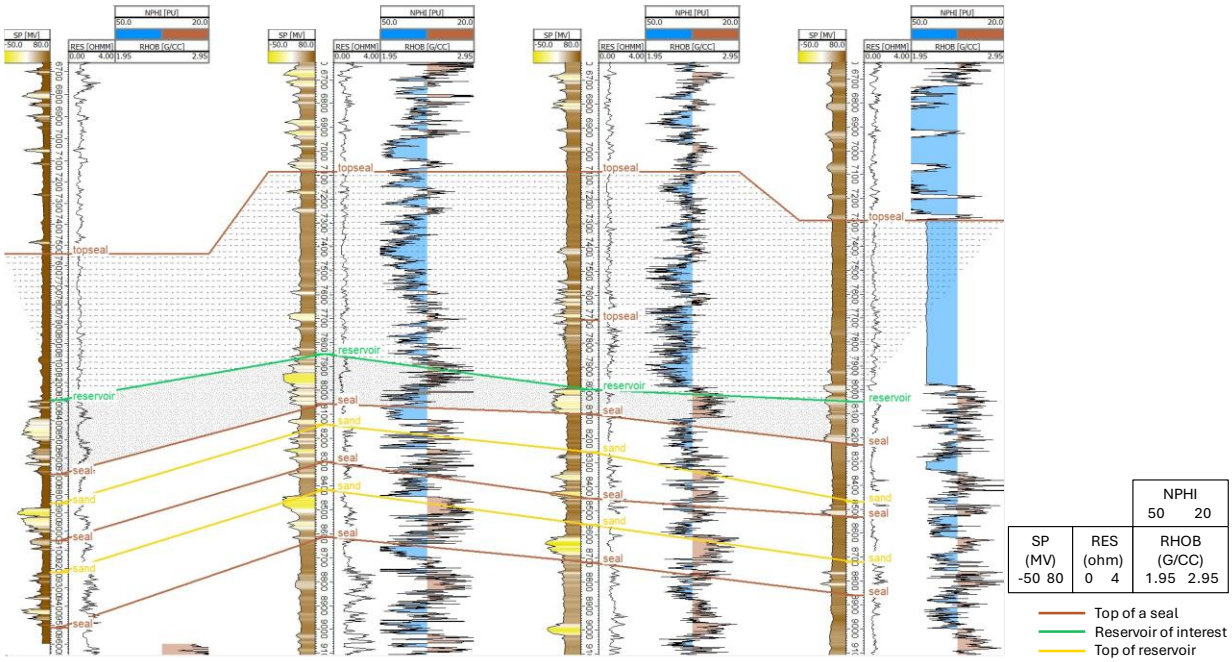

Figure 8. Selected wells from well log interpretation displaying stacked saline aquifers; shallow-most aquifer is the reservoir used for this study.

Logs narrow down surface area of interest to ninety-two square miles and seismic focus to 0-3 seconds, or depths below 2,600 ft to allow CO_2 to be in supercritical phase and above 10,000 feet to avoid geopressure. Using the SP and RES logs, multiple stacked and laterally continuous reservoirs (saline aquifers) of various thicknesses and their respective caprocks are identified at depths of ~7,900 ft (Figure 8). The shallowest reservoir of interest (shaded in Figure 8) from these is chosen to conduct this study as it is the thickest and to avoid overpressure. The caprock is part of the *Robulus "L"*, and is ~7,000 ft deep with a thickness of 700-1,000 ft. The reservoir is part of the *Discorbis "B"* formation, has a ~200 ft average thickness at a depth of 7,900 feet. These logs helped identify where the biomarkers, sealing layer, and reservoir are found for horizon mapping (Figure 6).

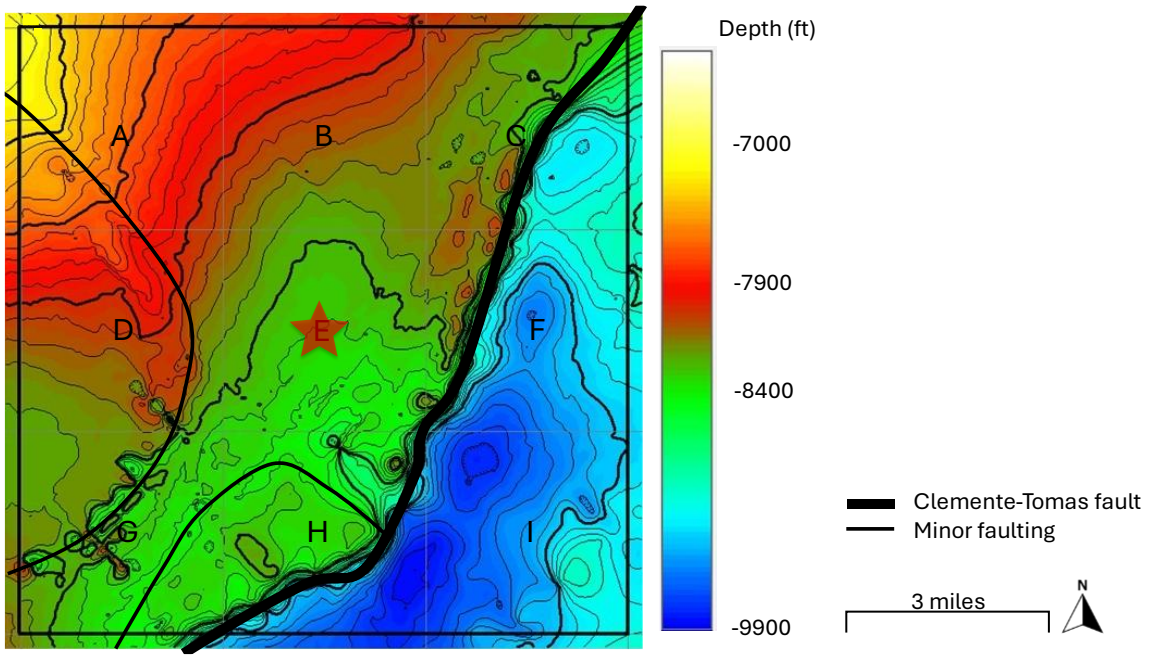

Figure 9. Structure map for the top of the storage reservoir (green horizon in Figure 6).

Dynamic CO_2 Storage Model

Models and simulations can help understand how CO_2 injections behave over time, by creating a geological model and using properties from data available. In this study, we evaluate the feasibility of geological carbon storage in the Matagorda Island leasing area, by testing multiple injection rate scenarios over a 30-year period. We present how a 3D seismic reflection survey and legacy wells are used to identify a potential Miocene saline aquifer for storage in the Matagorda Island leasing area, offshore Texas. Model and simulations test multiphase fluid flow for nine leasing blocks near the Clemente-Thomas fault to understand CO_2 changes in pressure and migration towards legacy wells or the Clemente-Tomas fault.

Seismic interpretations and mapping were exported from Kingdom into PetraSim to discretize the geologic model into a solution mesh for simulating four different CO_2 injection rates. This allowed properties, initial conditions, grid cells, and boundaries to be set. The dynamic CO_2 storage model created for this study requires a geologic conceptual model that is transformed through steps and assumptions into a digital representation of the study area of the

nine leasing blocks. This section describes model development, along with a discussion of assumptions of data sources for the modeling process.

Conceptual Model

The model consists of 5 main components, the overburden, seal (~700 feet average thickness), reservoir (~200 feet average thickness), under-burden (undifferentiated formations that occur beneath the target reservoir), and the Clemente-Tomas fault (Figure 10). The coordinates for the seal & reservoir and the Clemente-Tomas fault layers are set to 0,0 origin to de-identify the location of the nine leasing blocks, each being 3×3 miles. The lateral extent of the model domain is 14,484×14,484 meters (9×9 miles), with depths from 0 through 3,000 meters (9,843 feet) below the mudline. The seal and reservoir horizons mapped from Kingdom are the basis of the rest of the model. The overburden starts at a depth of 0 meters and lies above the seal. Then, the seal and reservoir layers follow. The underburden lies beneath the reservoir until a depth of 3,000 m. While minor faulting is found in the seismic data, only the Clemente-Tomas fault is included as an internal boundary inside the model to maintain simplicity, as this is a pre-feasibility analysis designed to test proof-of-concept. Fourteen legacy wells in these leasing blocks are plotted from data available from GeoTomo and BOEM.

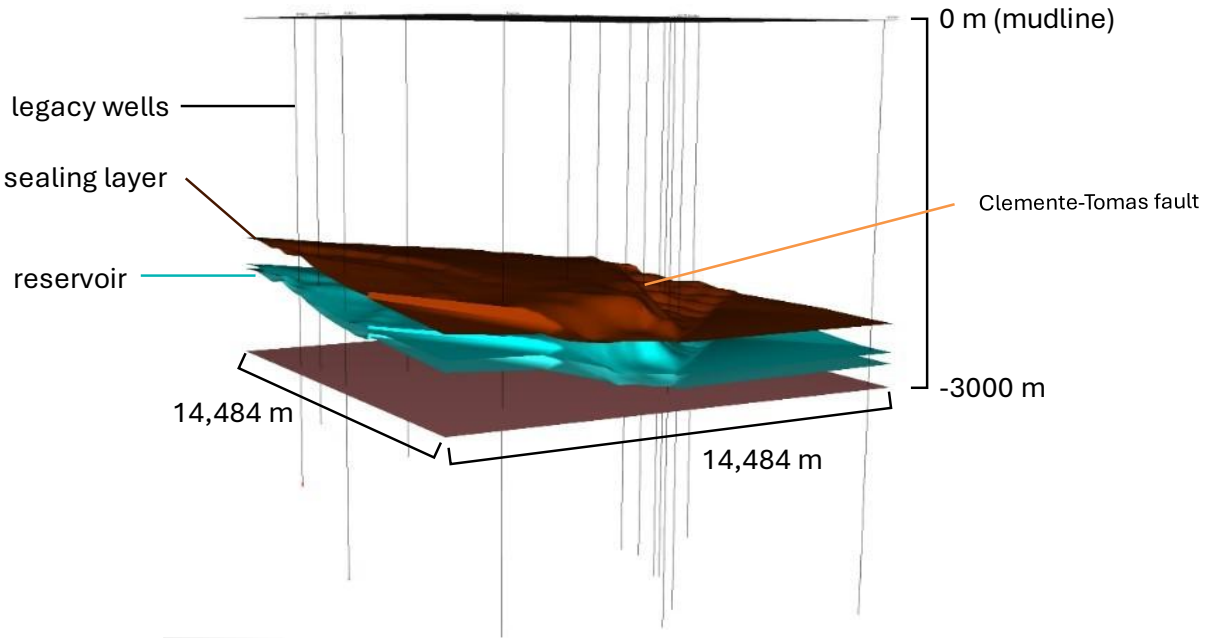

Figure 10. Conceptual model layers with a 4x vertical exaggeration.

Model Properties

Using the BOEM Sands dataset, data from three chronozones, the Upper Lower Miocene (MUL), the Middle Lower Miocene (MML) and the Lower Lower Miocene (MLL), is taken to analyze relationships between porosity and permeability for sands. For depths of 7,000-9,000 feet (depths of Lower Miocene sands ranging from the reservoir depth to geopressure) the mean porosity is 0.27 and mean permeability is 217 mD for sands (Figure 4, Figure 5). Density, wet heat conductivity, and specific heat values are assigned following (Robertson, 1988). Because the fault is sealing, the same low porosity and permeability values from the seal are assigned to the fault for modeling.

	Density (kg/m^3)	**Porosity**	**XY Permeability** (m^2)	**Z Permeability** (m^2)	**Wet Heat Conductivity** (W/m-K)	**Specific Heat** (J/(kg-K))
Overburden	2,600	0.1	2.14×10^{-13}	1×10^{-15}	2.0	1,000
Sands	2,650	.27	2.14×10^{-13}	2.14×10^{-13}	5.0	730
Shale	2,600	0.1	1×10^{-18}	1×10^{-18}	3.0	1,270
Underburden	2,600	0.1	2.14×10^{-13}	1×10^{-15}	2.0	1,270
Fault	2,600	0.1	1×10^{-18}	1×10^{-18}	3.0	1,000

Table 1. Properties set for model.

Initial & Boundary Conditions

Initial conditions comprise a single fluid phase (brine), which is specified with initial pressure, temperature and salt mass fraction. The initial pressure gradient, *P(*z), is modeled as a function of depth (*z*) with the expression: $P(z) = 3.03 \times 10^5$ Pa + $(1.0894 \times 10^4$ Pa $m^{-1})$ z, where 3.03×10^5 Pa is fluid pressure at seafloor, assuming 30 m water column, and the pressure gradient of 1.089×10^4 Pa m^{-1} reflects hydrostatic conditions, following (Burke et al., 2012). Similarly, the depth-dependent temperature gradient, *T*(*z*) is modeled as, $T(z) = 5°C + (0.033$ °C $m^{-1})$ z, using initial temperatures and subsea depth from BOEM well data in the leasing blocks. Salt mass fraction is set to 0.119, as studies from (Yang et al., 2014) indicate that brine salinity within the Gulf of Mexico Miocene sands is ~119,000 mg/L ppm TDS. The seafloor and lateral extent of the model domain are specified as constant pressure and temperature boundaries to maintain the seafloor pressure and temperature conditions, as well as the far-field pressure and temperature gradients throughout the duration of the simulation. The base of the model is a no-flow boundary.

Code Selection & Grid Discretization

This study implements PetraSim (RockWare, 2024) to convert the geologic model into a simulation grid comprising 147,200 grid cells. The grid is discretized in the horizontal plane by Voronoi tessellation, which results in polygonal (4, 5, and 6 sided) grid cells with near-orthogonal connections, the result of which reduces discretization error that occurs when radial flow is simulated within a Cartesian grid.

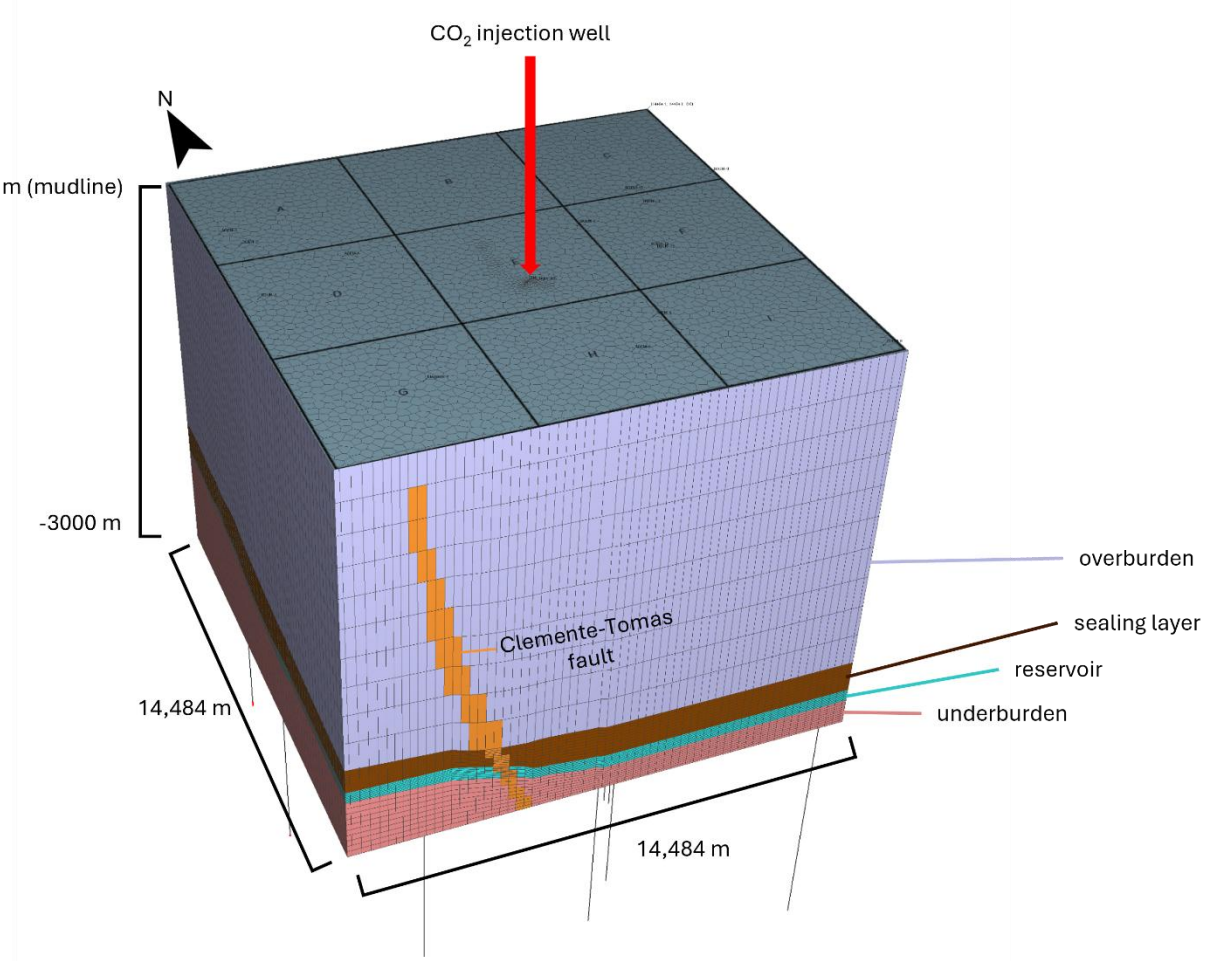

Figure 11. Grid discretization in PetraSim.

CO_2 injection is simulated using the TOUGH 3.0 (Jung et al., 2017) compiled with equation of state ECO2N. The TOUGH 3.0/ECO2N code solves mass and energy conservation equations for heat and fluid flow, while considering the multiphase, multicomponent fluid flow processes that occur during CO_2 storage in saline aquifers. Specifically, the ECO2N module implements the equation of state for nonisothermal mixtures of H2O, CO_2, and NaCl, including solid phase NaCl precipitation. To record CO_2 saturation and fluid pressure changes at specific locations along the fault, monitoring locations are specified using the "FOFT" feature of the TOUGH 3.0 simulator. This feature stores temperature, pressure, and CO_2 saturation for each timestep during the simulation run and thus emulates data that may be collected from monitoring

wells located within the domain. A total of five monitoring (FOFT) locations are specified within the top layer of the reservoir as illustrated in Figure 12.

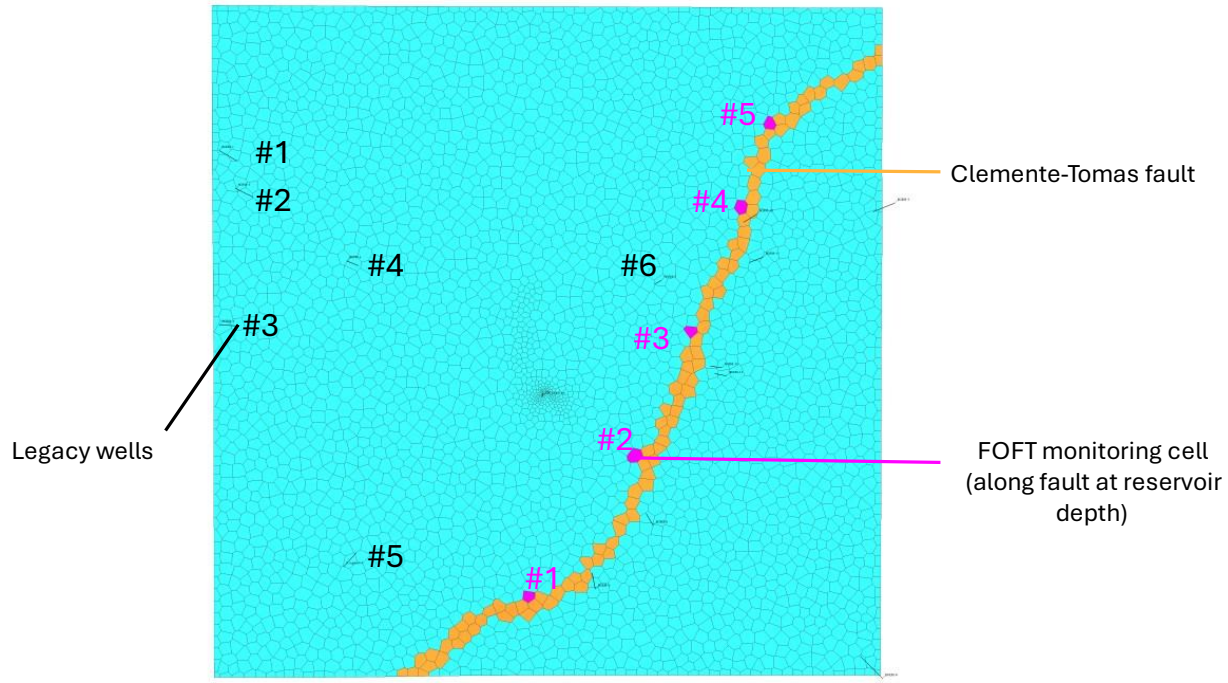

Figure 12. FOFT monitoring cells (purple polygons) are located within the upper reservoir and along Clemente-Tomas Fault.

Model Scenarios

Using the model described, four different CO_2 injection scenarios are assessed, with a goal to inject 30 MMT, 50 MMT, 100 MMT, and 150 MMT of CO_2 over a 30-year period. These injection rates are chosen because they could be feasible on a commercial scale. A total of 30 MMT of CO_2, is a rate of 1 MMT/year, which is the minimum amount injected by the Sleipner project (Chadwick & Eiken, 2013; Korbøl & Kaddour, 1995; Solomon, 2007). The second scenario is developed after the NETL's Carbon Storage Assurance Facility Enterprise (CarbonSAFE) project aim for developing storage sites with a minimum target of 50 MMT of CO_2 over a 30 yr period, or 1.7 MMT/yr (Rosen et al., 2024; Sullivan et al., 2020). The third and fourth scenarios consist of storage rates are double and triple the rate of the 50 MMT of CO_2 stored. Over a 30-year period, these simulations are set to inject into five cells in the *Discorbis*

"B" formation, at a depth of 2,486 m, on leasing block E. For discussion purposes the three CarbonSAFE scenarios are denoted as CarbonSAFE1 (50 MTT in 30 yrs), CarbonSAFE2 (100 MMT in 30 yrs) and CarbonSAFE3 (150 MMT in 30 yrs).

Caprock, reservoir and fault layers are imported into ParaView. CO_2 simulation results are visualized by converting the XYZ data into points, using the table to points filter and the 3D Delaunay triangulation filter to display the extent of the model. Isosurface contours are created to image CO_2 saturation and change in pressure in 3D.

Results and Discussion

This study assessed the amounts of CO_2 that could be safely stored by using one well, over a 30-year period, without having high pressures along the Clemente-Tomas fault and the CO_2 not migrating towards the fault or nearby legacy wells. Five monitoring cells placed on the reservoir top along the fault (Figure 12) using the FOFT print option to record changes in pressure over every time step of the injection. A common trend between all injections is pressure change (dP) increasing the most at the start of the injection period at years 0-5 and slowly stabilizing until the end of the 30-year period. Simulations from the 1 MMT/year and the CarbonSAFE1 scenario show the CO_2 was stored without reaching the Clemente-Tomas fault (Figure 14, Figure 18) and CO_2 plume diameters being <3 miles (Figure 15, Figure 19). While visualization in ParaView for the CarbonSAFE2 and CarbonSAFE3 scenarios show the CO_2 plume reaches the fault, as seen with the irregular plume shape (Figure 22, Figure 26), numerical results show there is no CO_2 at the fault monitoring cells; this could be due to the low fault porosity-permeability values set as seen in Table 1. The CO_2 plumes in both these scenarios have a diameter >3 miles (Figure 23, Figure 27).

FOFT print options are used for the legacy wells included in the model. From 14 legacy wells, 7 are included in ParaView visualizations, and 3 of them, wells #4, #5, and #6, are chosen

for further dP analysis, as those are closest to the injection site and have the highest risk to have the CO_2 plume expand towards them. Throughout all scenarios, CO_2 does not reach the grid cell at legacy well #6. Results from the 4 injection scenarios show that dP is greatest in well #6, with a minimum of 0.33 MPa for the 1 MMT/year injection scenario, and a maximum of 1.1 MPa at the CarbonSAFE3 scenario (Figure 17, Figure 29). The pressure increase required to cause a fault to slip varies; however, previous studies have shown that an increase of 1 MPa is enough to initiate slip (Dvory et al., 2022; Koehn, et al., 2023b), making the CarbonSAFE3 scenario the least promising.

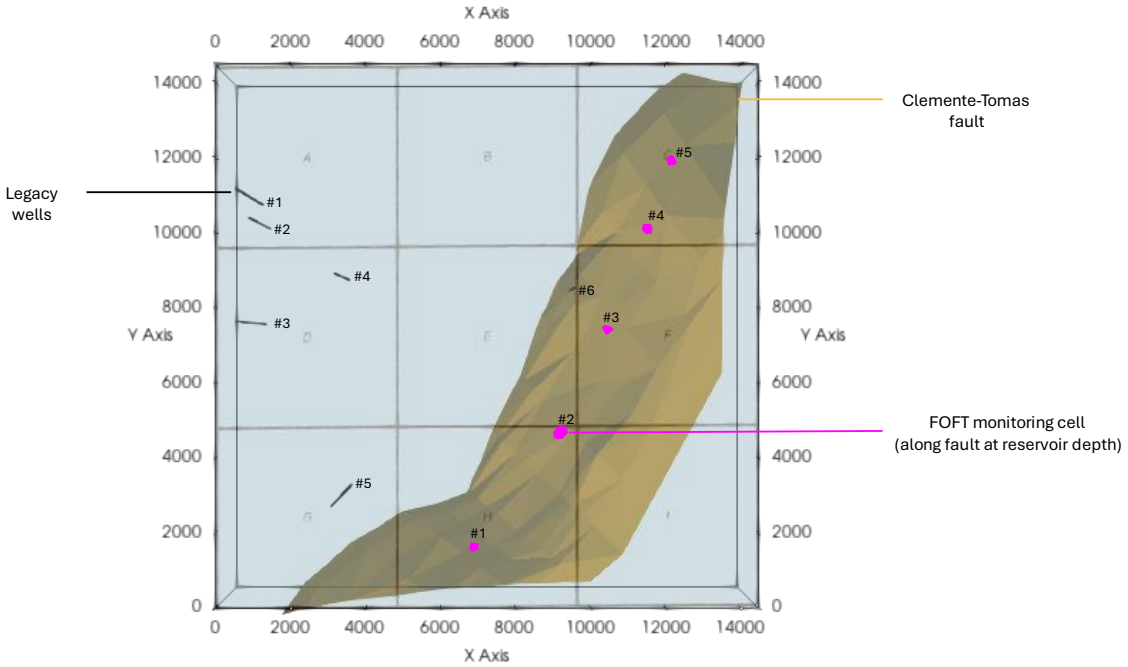

Figure 13. Six legacy wells (black lines) and FOFT monitoring cells (pink polygons) in the study area. Brown shading denotes fault surface – this convention is used in all subsequent simulation figures.

1 MMT

In the first injection scenario of 1 MMT/year, the CO_2 plume did not reach the Clemente-Tomas fault or any legacy wells (Figure 14). Figure 15 shows the plume had a diameter of ~3,670 meters (~2.3 miles), expanding throughout the majority of leasing block E, and into the edge of block H. FOFT cell #3 on the fault experienced a maximum dP at 0.30 MPa (Figure 16), and legacy well #6 had dP of 0.33 MPa at the end of the 30-year period (Figure 17). The lateral extent of the CO_2 plume for this injection scenario suggests that selecting an injection location closer to the center of leasing block E is likely to keep the CO_2 entirely within a single leasing block.

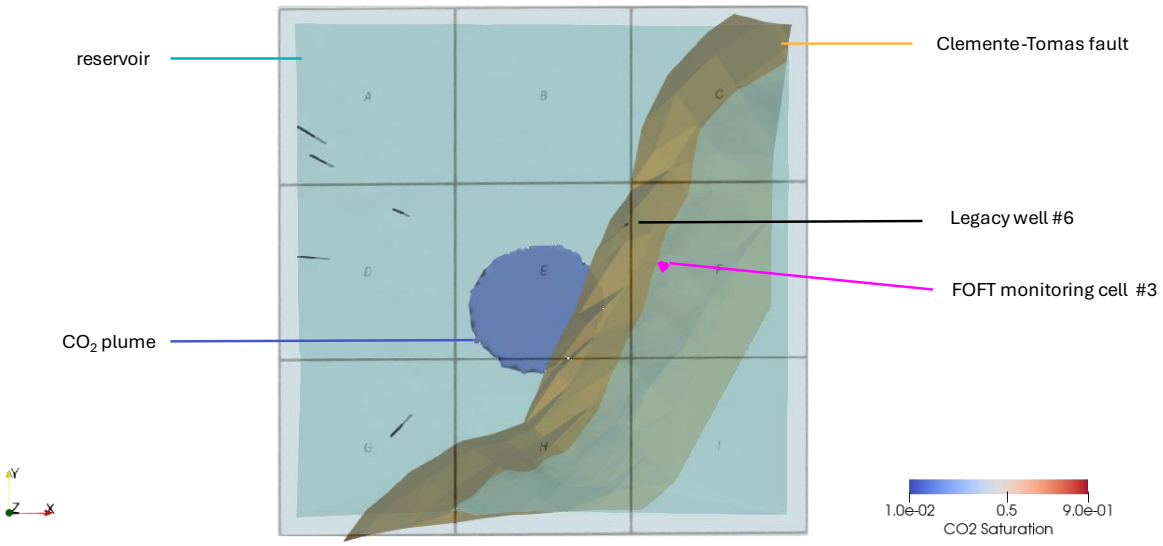

Figure 14. CO_2 plume expansion after 30 years at a rate of 1 MMT/year.

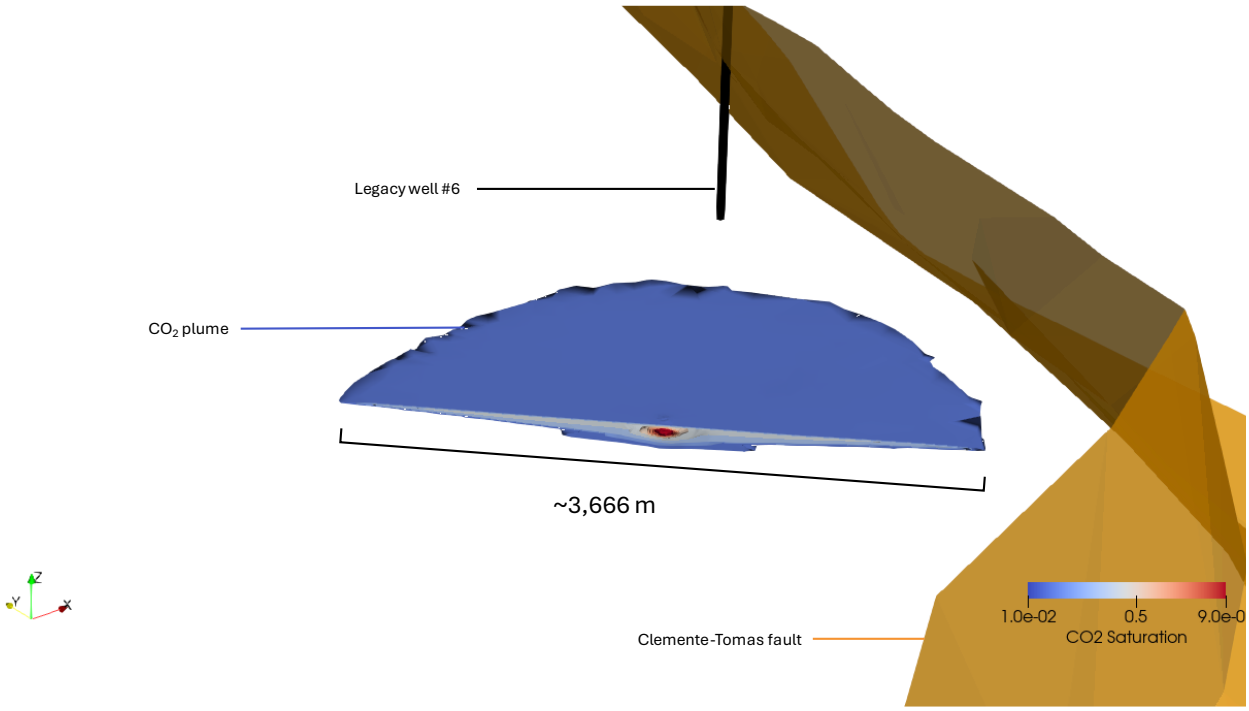

Figure 15. Cross section view of 1 MMT/year CO_2 plume after 30 years.

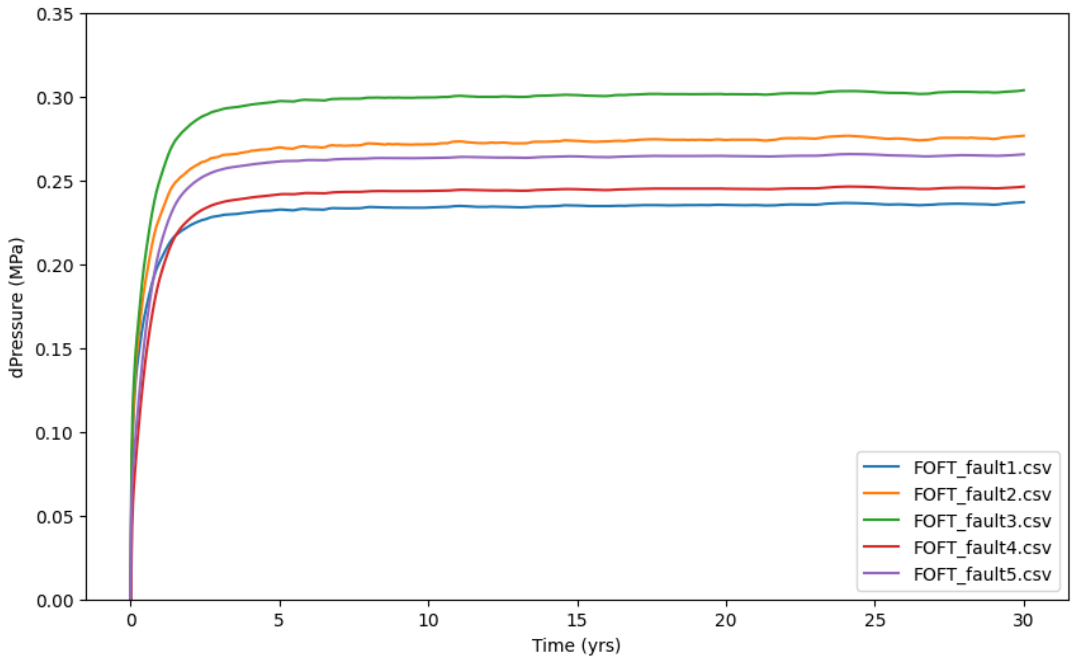

Figure 16. Fault dP at 1 MMT/year for 30 years.
Monitoring locations for each FOFT cell are shown in Figure 12.

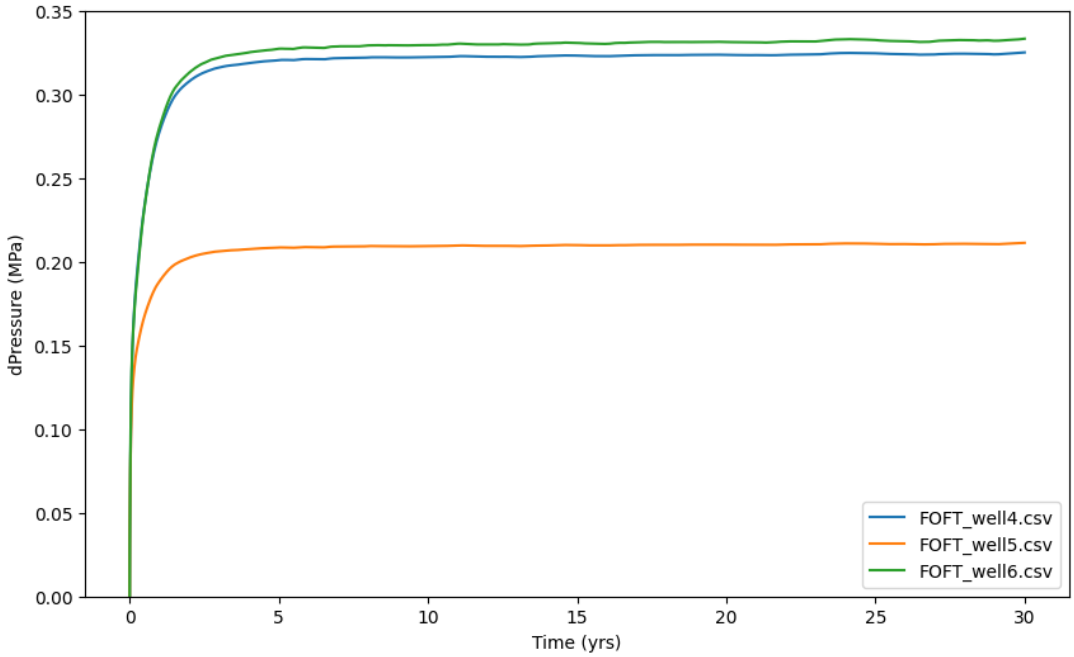

Figure 17. Legacy wells dP for 1 MMT/year injection. Well locations are shown in Figure 13.

CARBONSAFE 1

For the CarbonSAFE1 scenario of 1.7 MMT/year, the CO_2 plume approaches the Clemente-Tomas fault but does not appear to intersect the fault zone (Figure 18, Figure 19); however, the close proximity suggests that more detailed geologic characterization may be required to assess permeability along the damage zone of the fault. The CO_2 plume has a diameter of ~4,510 meters (~2.8 miles). These results also show that the CO_2 plume remained far from legacy wells, suggesting that wellbore leakage is minimal risk. Nevertheless, the CO_2 plume expanded throughout the majority of leasing block E, into block H, and begins to enter block D at the D/E block border. At the end of this scenario, FOFT cell #3 along the fault, experienced the highest dP at ~0.43 MPa (Figure 20), and legacy well #6 dP was ~0.46 MPa (Figure 21). The expanded footprint of this CO_2 plume suggests that multiple leasing blocks may be necessary for lateral containment.

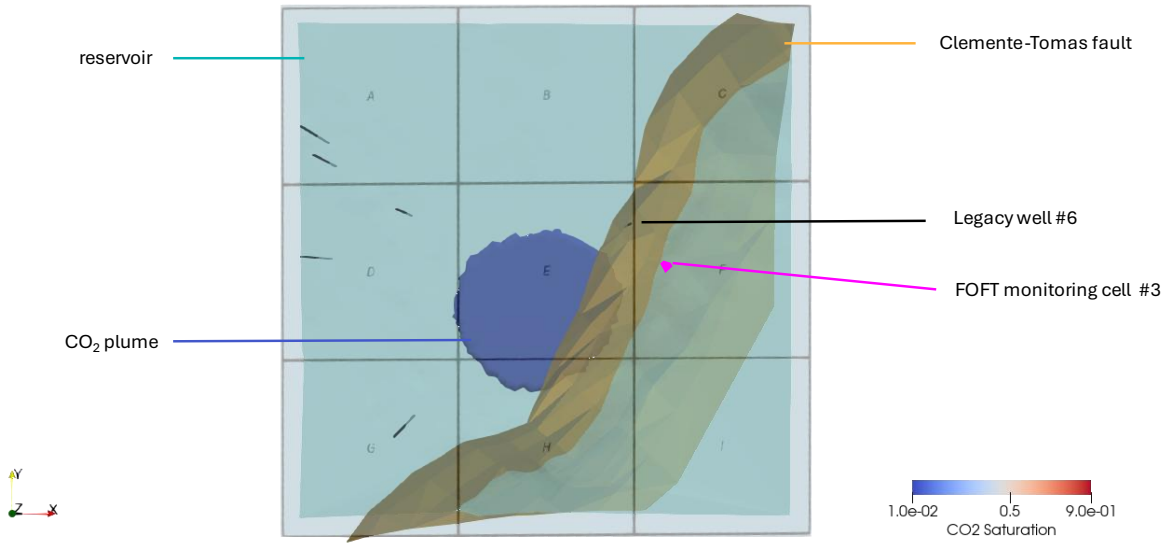

Figure 18. CO_2 plume expansion after 30 years at a rate of 1.7 MMT/year.

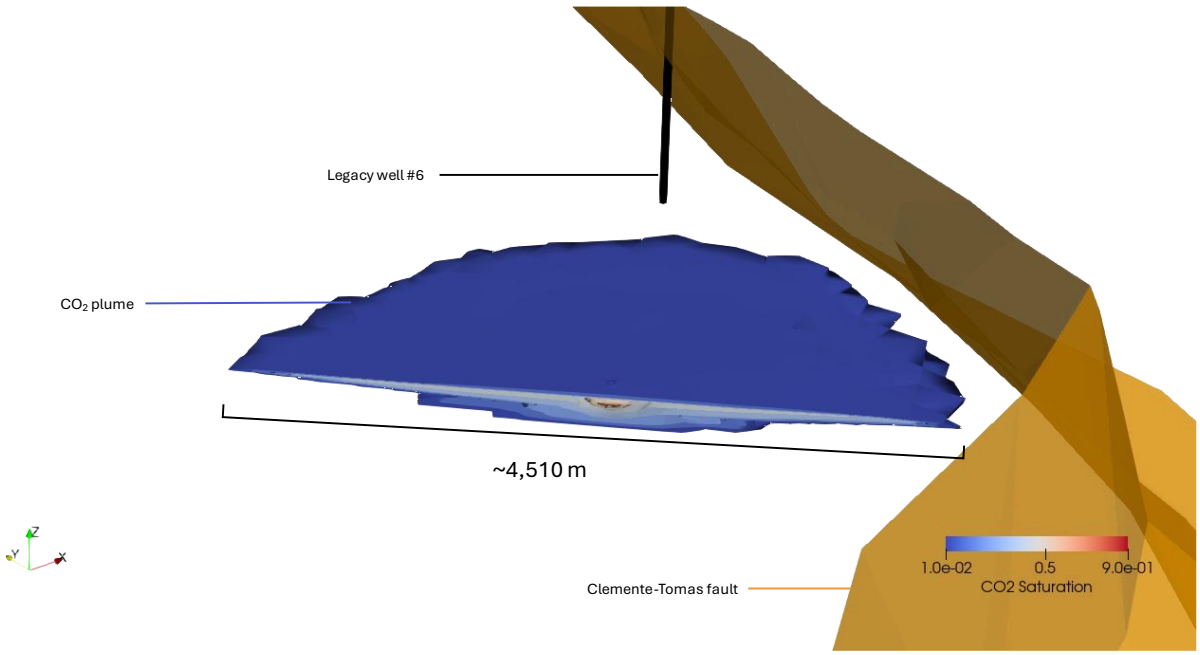

Figure 19. Cross section view of 1.7 MMT/year CO_2 plume after 30 years.

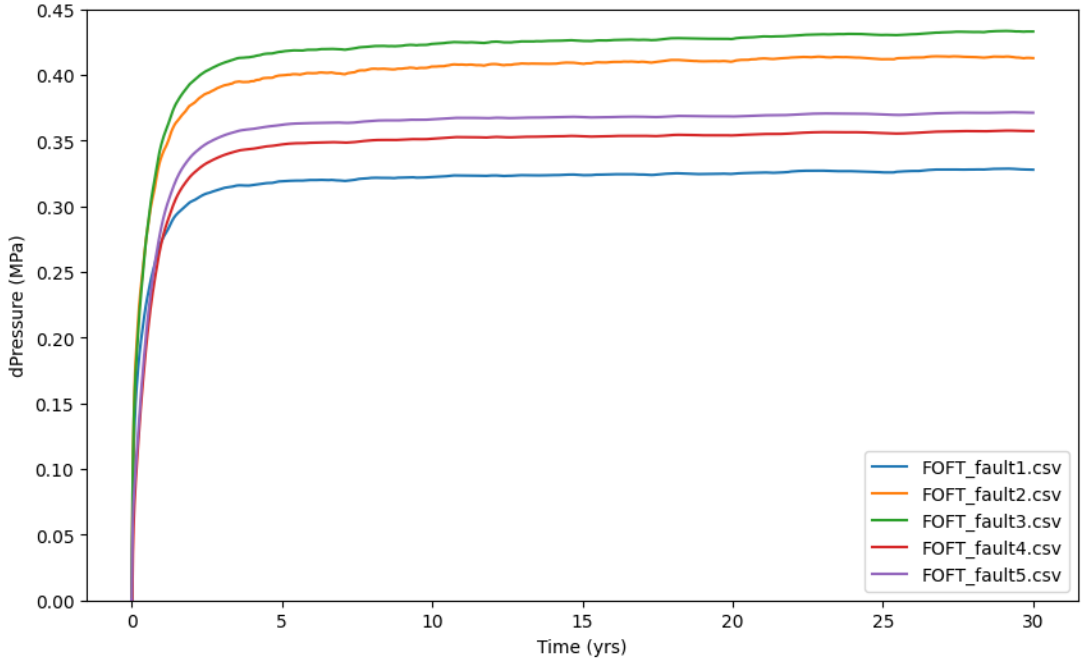

Figure 20. Fault dP at 1.7 MMT/year for 30 years.
Monitoring locations for each FOFT cell are shown in Figure 12.

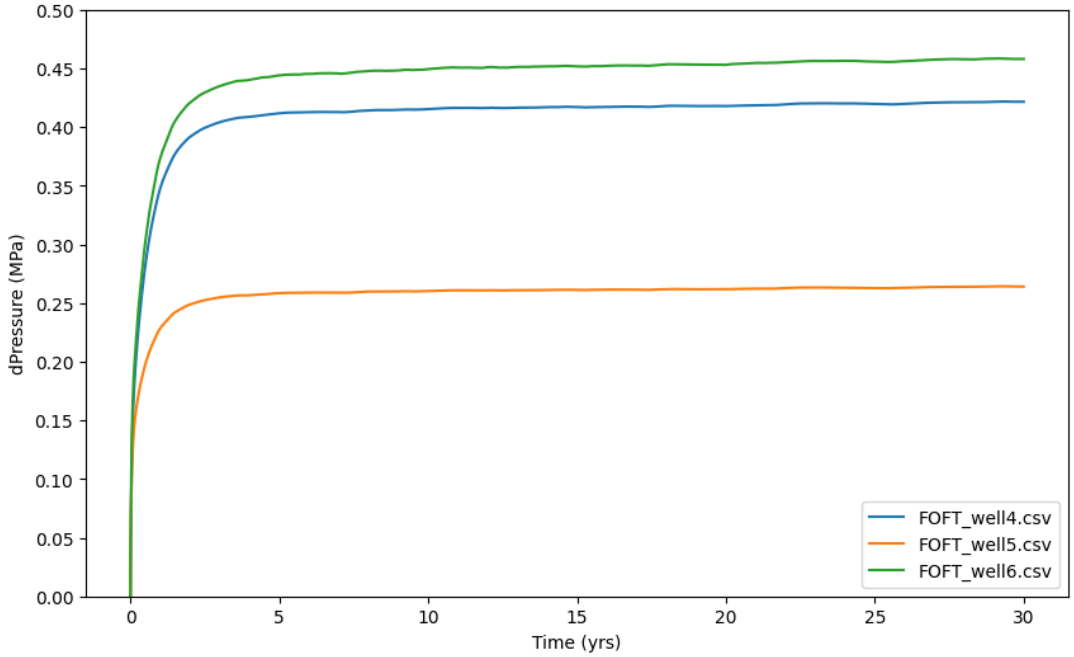

Figure 21. Legacy wells dP for 1.7 MMT/year injection.
Well locations are shown in Figure 13.

CARBONSAFE 2

In the third injection rate of 3.4 MMT/year, Figure 22 and Figure 23 show the CO_2 plume has a diameter of ~5,390 meters (~3.35 miles) and begins building up at the Clemente-Tomas fault and starts getting closer to legacy well #6. Here, it expanded through over three quarters of leasing block E, part of block H (which has the Clemente-Tomas faulting through it from SW-NE direction), and enters block D from the east. dP from FOFT cells shows that fault FOFT cell #2 and #3, experience the highest changes in pressure at ~0.76 and ~0.77 MPa, respectively (Figure 24). Throughout year 0-25, the dP at fault #2 is the highest. At ~year 25, fault FOFT cells #2 and #3 are the same, and dP at FOFT cell #3 remains the highest until the end of the 30-year period. dP for legacy well #6 is ~0.78 MPa by the end of the simulation (Figure 25).

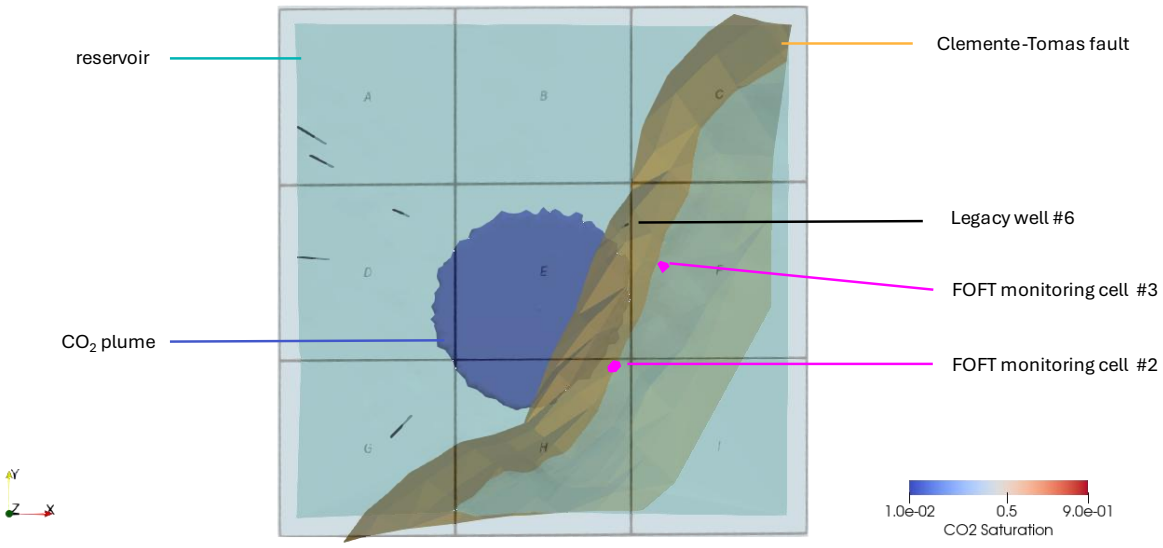

Figure 22. CO_2 plume expansion after 30 years at a rate of 3.4 MMT/year.

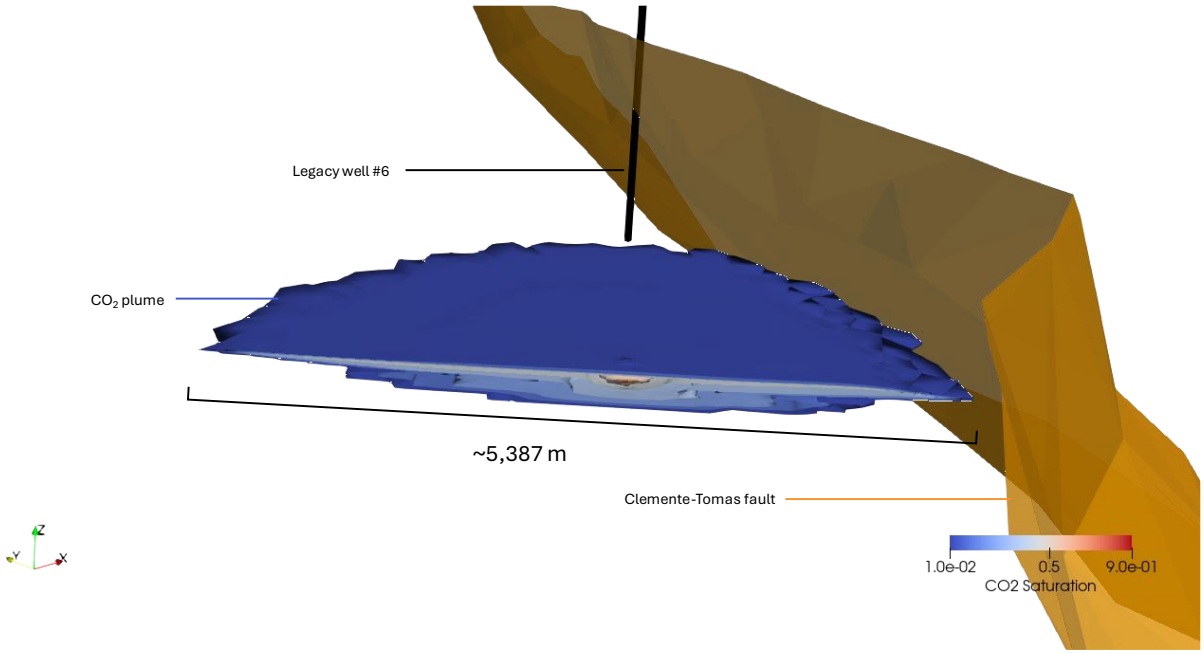

Figure 23. Cross section view of 3.4 MMT/year CO_2 plume after 30 years.

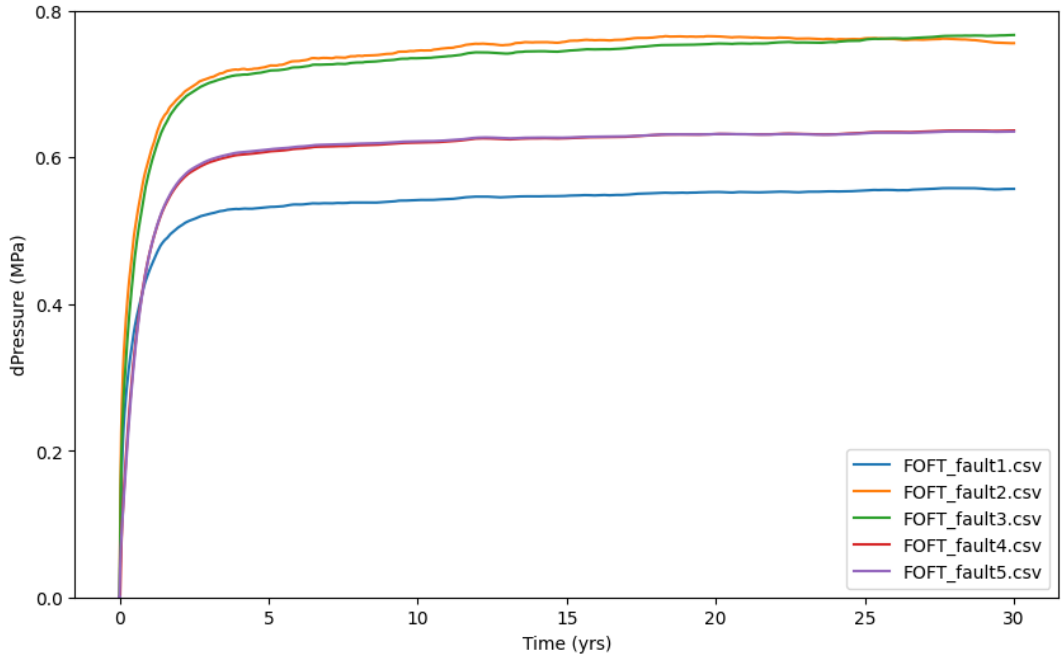

Figure 24. Fault dP at 3.4 MMT/year for 30 years.
Monitoring locations for each FOFT cell are shown in Figure 12.

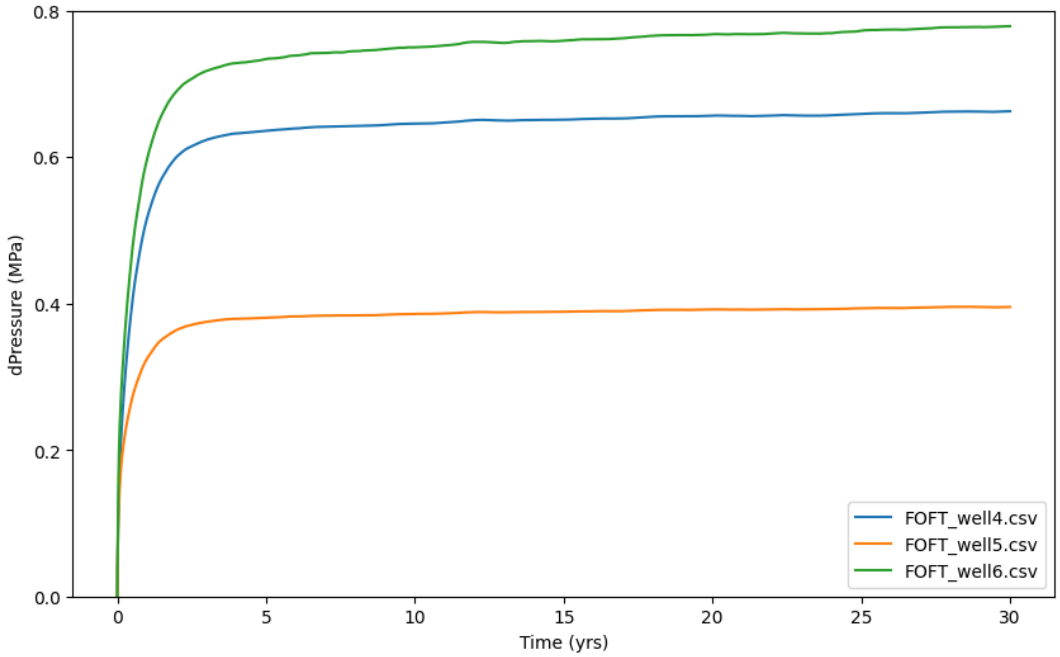

Figure 25. Legacy wells dP for 3.4 MMT/year injection. Well locations are shown in Figure 13.

CARBONSAFE 3

The fourth injection with a rate of 5.1 MMT/year, resulted in the CO_2 plume having a diameter of ~5,720 meters (~3.55 miles) and noticeable build up against the Clemente-Tomas fault while reaching closely to legacy well #6 (Figure 26, Figure 27). Here, the plume expands over leasing blocks E, D, H, and into the corner of block G. The dP from fault FOFT cells shows that FOFT cell #2 and #3, experience the highest changes in pressure at ~1.1 MPa (Figure 28). FOFT cell #2 experienced the highest from the start of injection up until ~year 27, where dP for cell #2 and #3 is the same, and dP at FOFT cell #3 slightly increases over FOFT cell #2 at the end of the 30-year period. At legacy well #6, dP also reaches 1.1 MPa at the end of the 30 years (Figure 29).

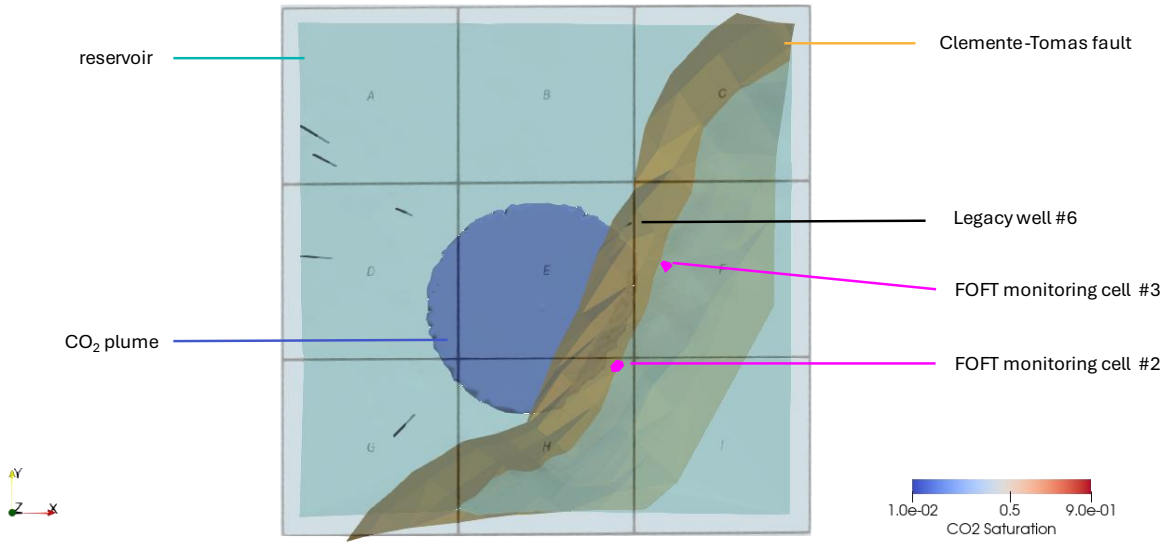

Figure 26. CO_2 plume expansion after 30 years at a rate of 5.1 MMT/year.

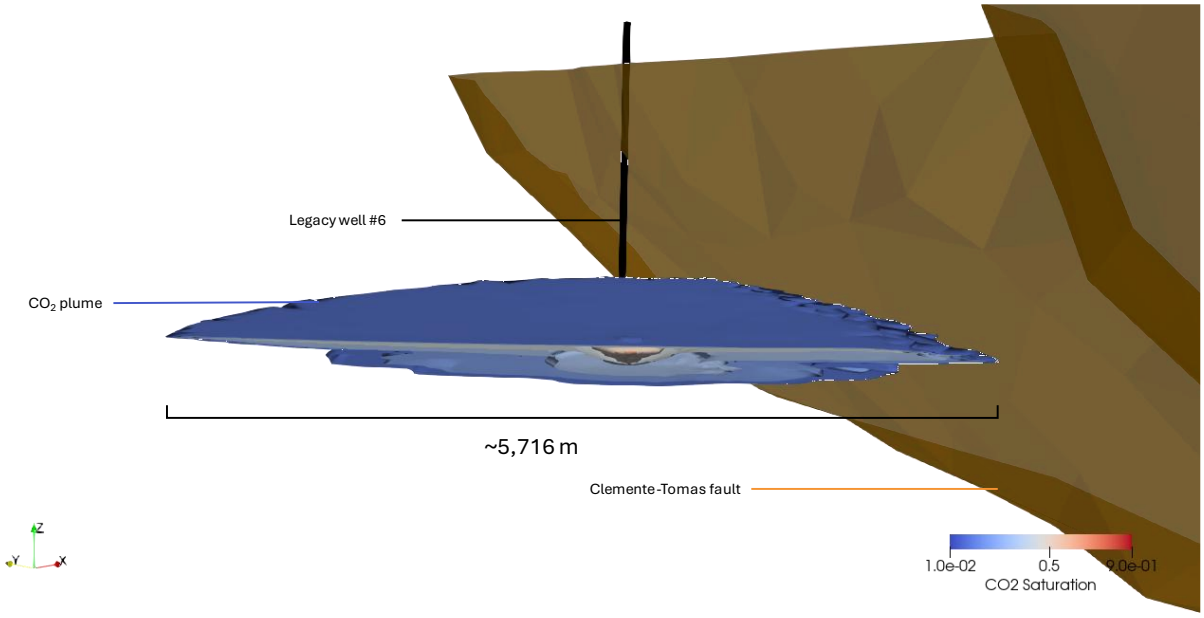

Figure 27. Cross section view of 5.1 MMT/year CO_2 plume after 30 years.

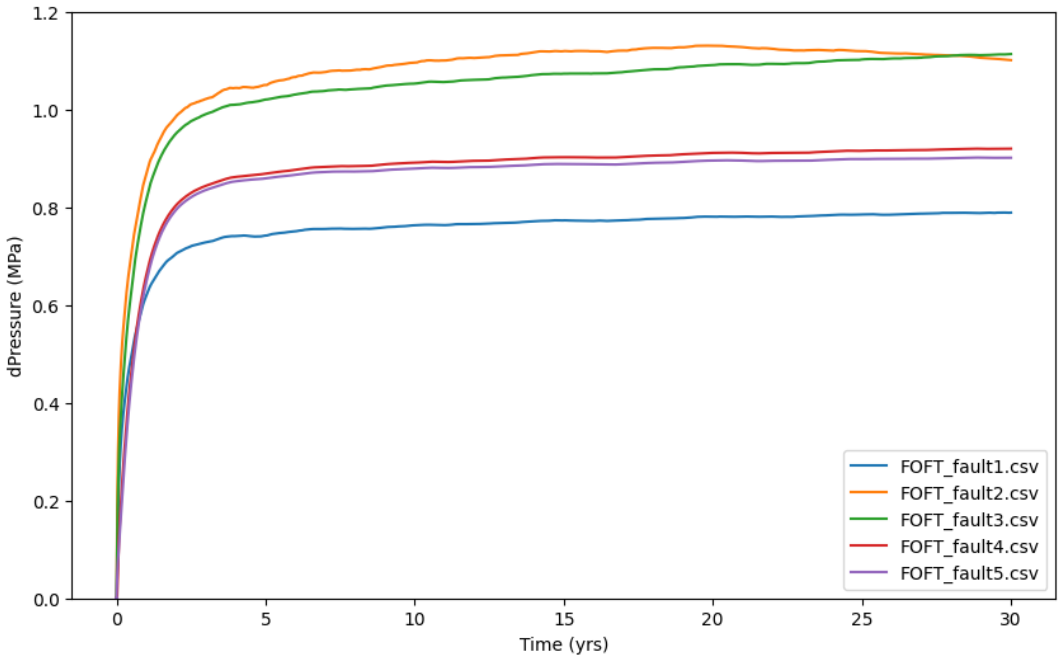

Figure 28. Fault dP at 5.1 MMT/year for 30 years.
Monitoring locations for each FOFT cell are shown in Figure 12.

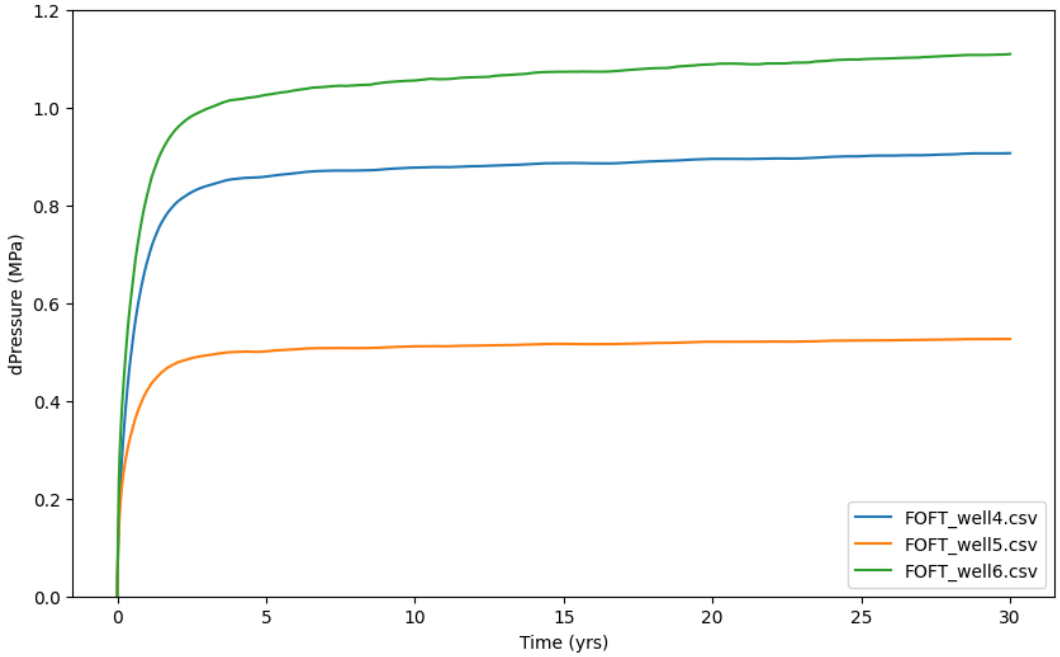

Figure 29. Legacy wells dP for 5.1 MMT/year injection.
Well locations are shown in Figure 13.

Risks and Monitoring

Although CCS can help with the removal and storage of CO_2 emissions, these projects require caution as early as the pre-injection stage to monitor efforts during and after injection to mitigate geological risks, such as induced seismicity or leakage through legacy wells. Pressures and temperatures, injection rates, reservoir and caprock quality, legacy well integrity, and CO_2 transport are key factors to consider in carbon storage projects for environmental safety and monitoring.

Subsurface risks and uncertainties

Pore Space and Leasing Rights

A consideration before the injection phase is pressure space, or pore volume times pressure. While many CCS projects are considered on pore space available, pressure build-up is a limit to the CO_2 storage capacity (Bump & Hovorka, 2024). Multiple projects in close proximity to one another could increase pressure barriers from one another, limiting how brine is displaced (Bump & Hovorka, 2024). From each of these scenarios, CO_2 plumes expanded into other leasing blocks. As carbon storage projects develop, understanding the CO_2 plume footprints is important to know which leasing bocks projects must account for in their monitoring efforts.

Legacy Wells

In this study, higher injection rates resulted in greater pressure increases along the fault and at legacy well #6, with a maximum of 1.1 MPa. Changes in pressure from simulations can help with understanding potential issues with injection location and rates that could trigger induced seismicity or leakage. In the Gulf of Mexico, there are 1.1 million legacy wells and active faults, which could be limiting to storage because wellbore integrity and pressure-induced fault slip pose a risk of induced seismicity or leakage (Bump & Hovorka, 2024; Tors et al., 2024). For example, CO_2 migrating into a legacy well that is not abandoned or plugged properly could be a leakage pathway (Tors et al., 2024). Knowing the condition of these wells, especially

if plugged, is necessary for long term CO_2 storage (Tors et al., 2024). If wells have been permanently plugged and abandoned, remediating them can be difficult, and negatively affect the reservoir (Tors et al., 2024). A challenge to characterizing well risks is their age, and lack of data or documentation of its construction, completion or history (Arbad et al., 2022; Tors et al., 2024). Although the wells could have been built and drilled to standard at the time, their construction did not consider CO_2 injection following after (Tors et al., 2024). Handling these legacy wells in potential CO_2 storage reservoirs is important to consider for areas like the Gulf of Mexico that were actively explored for decades (Koehn, et al., 2023b). Despite these risks, this study found that CO_2 did not reach any of the legacy well locations within the nine leasing blocks that comprise the study area, even when injection rates exceeded 3 MMT per year. As a result, this study demonstrates that CO_2 leakage from legacy wells is avoidable if injection wells are appropriately sited.

Caprock Integrity and Induced Seismicity

Caprocks, the low permeability layers overlying the reservoir, are meant to keep the CO_2 permanently contained and prevent the CO_2 from escaping. Its thickness, lateral extent, and integrity are a prerequisite for successful CO_2 containment (Kaldi et al., 2013). While some data can proof a caprock is sufficient for hydrocarbons, CO_2 injection could actually alter the caprock and sealing integrity (Busch et al., 2010; Paluszny et al., 2020). Caprocks can be affected by existing or future faults and fractures caused by changes in pressure, which could also result in CO_2 leakage. Caprock systems need to be assessed individually for each site including geomechanics on fault reactivation (Kaldi et al., 2011; Paluszny et al., 2020). Induced seismicity could compromise sealing capabilities, which could result in CO_2 leakage (Song et al., 2023; Vilarrasa et al., 2019). To prevent this, it is best to characterize fault systems and select a site further away from major faulting (Cheng et al., 2023). In 3D seismic surveys, faults over 5 km in

size are identifiable, while smaller faults ~1 km in length become harder to detect, making it challenging to have complete fault system characterization (Cheng et al., 2023). Complicated fault systems can make it difficult to predict induced seismicity from injections. However, recognizing faults within the caprock or reservoir is essential as they could impact its integrity.

Geomechanical seal properties can be affected by regional stress, existing faults, and fractures, which can be heightened by changes in pressure from injecting CO_2 (Kaldi et al., 2013). The pressure on the caprock can depend on the caprock permeability and the injection well location (Kaldi et al., 2013). Moreover, studies show that if a fault slipped, even if it was of low-permeability it could potentially be a conduit and increase fluid pressure, because permeability could quickly increase (Cappa et al., 2022). Results from this study showed legacy well #6 and FOFT cell #3 along the fault experienced the most increase in pressure. Simulation-based dP results can provide insight onto injection rate limits. While this study includes dP for the Clemente-Tomas fault and nearby legacy wells, it does not include minor faulting in the region that could affect the amount of CO_2 that can be stored.

Large-scale CO_2 can be safely stored by considering multiple factors that could be a risk such as faults, pressure build up, and CO_2 leakage through legacy wells. While monitoring and regulations have not been set in stone in the U.S., success in early CO_2 injection projects can help with regulations development, understanding best monitoring practices, and public perception.

Transportation

Safe transport is required for commercial-scale carbon sequestration and CO_2 transportation, efficiency of existing infrastructure, and associated costs must be considered. Infrastructure failure, corrosion or damage can result in leakage during transport (Ma et al., 2022; Mazzoldi et al., 2011). Pipelines offshore require more complicated construction than

onshore, and operate at higher pressures and lower temperatures than onshore pipelines (Smith et al., 2021). Studies show that offshore pipelines are more expensive than onshore, as much as 40-70% (Luo et al., 2023; Smith et al., 2021). The cost of pipelines can be influenced by its construction and operation costs, such as material, diameter, and length required to transport CO_2. While some studies have suggested utilizing existing pipelines, repurposing of some natural gas pipelines may not be feasible for transporting CO_2 of 20 Mtpa through distance of 100 miles or more (Smith et al., 2021). This challenge to repurpose existing pipelines occurs because of the highly corrosive nature of CO_2, which may result in pipeline failure in aging legacy infrastructure. Functional pipeline systems are essential for offshore storage and can be achieved through careful planning and design.

Model Limitations and Uncertainty

Uncertainties for this study included reservoir heterogeneity and restricting variability in hydraulic properties within the reservoir and fault zone. In the seismic survey, while some logs show a thick "clean" mud-dominated layer overlying the reservoir of interest, other logs show heterogeneity. At the well-log in leasing block D, interbedded, sandy layers are present with thicknesses as thin as 7 feet and up to 34 feet thick. While they are thin and not laterally extensive on the survey-scale, having baffles could be a risk for very slow CO_2 flow. Due to their thin size on the seismic-reflection scale, incorporating them into horizon mapping and modeling is a limitation. Heterogeneity affects porosity and permeability, affecting CO_2 flow (Gao et al., 2023). In this study, porosity and permeability values were assigned for the reservoir based on chronozone and depth from BOEM, however, these values were collected from well-specific locations and do not account for variability in porosity and permeability in between these locations. Previous studies, show that permeability heterogeneity increasing decreased the

reservoir storage capacity; on the other hand, porosity heterogeneity increased capacity (Sohal et al., 2021).

Conclusions

This pre-feasibility assessment of CO_2 storage shows CO_2 storage potential in the Matagorda Island Leasing Area, in an offshore Lower Miocene saline aquifer. Seismic interpretation and legacy well-logs helped identify a ~200-foot-thick reservoir, and a ~1000-foot-thick seal that could be suitable for CO_2 storage. Properties reported from BOEM, and published literature are incorporated into our study for modeling and simulation. Simulations of the 1 MMT/year and 1.7 MMT/year, or a total of 30 MMT and 50 MMT over a 30-year period, at this initial stage of research appear promising. The 3.4 and 5.1 MMT/year rates are not feasible for a single injection well, as the simulations show that the CO_2 migrates towards the fault and experience changes in pressure of up to 1.1 MPa, enough to slip. Nevertheless, higher injection rates may be feasible in a stacked reservoir configuration, thus allowing multiple storage reservoirs to be accessible from a single offshore platform. Future work could include mapping minor faulting present in the survey and incorporating reservoir heterogeneity into models to further consider factors that could impact success of CO_2 storage. While CCS projects are rapidly being considered in the Gulf coast, there are not any in the Matagorda Island leasing area or at federal waters of the Gulf of Mexico. We hope characterization and simulations from this pre-feasibility study support further interest in feasibility studies to decarbonize industrial metro areas, such as Corpus Christi and Victoria.

Bibliography

Ajiboye, O., & Nagihara, S. (2012). STRATIGRAPHIC AND STRUCTURAL FRAMEWORK OF THE CLEMENTE-TOMAS AND CORSAIR GROWTH FAULT SYSTEMS IN THE TEXAS CONTINENTAL SHELF.

Alnes, H., Eiken, O., Nooner, S., Sasagawa, G., Stenvold, T., & Zumberge, M. (2011). Results from Sleipner gravity monitoring: Updated density and temperature distribution of the CO2 plume. Energy Procedia, 4, 5504–5511. https://doi.org/10.1016/j.egypro.2011.02.536

Arbad, N., Watson, M., & Heinze, L. (2022). Risk matrix for legacy wells within the Area of Review (AoR) of Carbon Capture & Storage (CCS) projects.

Arts, R., Eiken, O., Chadwick, A., Zweigel, P., Van Der Meer, L., & Zinszner, B. (2004). Monitoring of CO2 injected at Sleipner using time-lapse seismic data. Energy, 29(9–10), 1383–1392. https://doi.org/10.1016/j.energy.2004.03.072

Bandilla, K. W. (2020). Carbon Capture and Storage. In Future Energy (pp. 669–692). Elsevier. https://doi.org/10.1016/B978-0-08-102886-5.00031-1

Bashir, A., Ali, M., Patil, S., Aljawad, M. S., Mahmoud, M., Al-Shehri, D., Hoteit, H., & Kamal, M. S. (2024). Comprehensive review of CO2 geological storage: Exploring principles, mechanisms, and prospects. Earth-Science Reviews, 249, 104672. https://doi.org/10.1016/j.earscirev.2023.104672

Bump, A. P., & Hovorka, S. D. (2024). Pressure space: The key subsurface commodity for CCS. International Journal of Greenhouse Gas Control, 136, 104174. https://doi.org/10.1016/j.ijggc.2024.104174

Bureau of Ocean Energy Management (BOEM). (2020). Atlas of Gulf of Mexico Gas and Oil Sands Data [Dataset]. https://www.data.boem.gov/Main/HtmlPage.aspx?page=2020sands

Bureau of Ocean Energy Management (BOEM). (2025a). Oil and Gas Energy Fact Sheet. BOEM. https://www.boem.gov/factsheet/oil-and-gas-energy

Bureau of Ocean Energy Management (BOEM). (2025b). ProtractionPolygonsClipped [Vector Digital Data]. https://bobson.maps.arcgis.com/apps/webappviewer/index.html?id=f41d5a4a43804946b9d53c5c7da78d2b

Burke, L. A., Kinney, S. A., Dubiel, R. F., & Pitman, J. K. (2012). REGIONAL MAP OF THE 0.70 PSI/FT PRESSURE GRADIENT AND DEVELOPMENT OF THE REGIONAL GEOPRESSURE- GRADIENT MODEL FOR THE ONSHORE AND OFFSHORE GULF OF MEXICO BASIN, U.S.A.

Busch, A., Amann, A., Bertier, P., Waschbusch, M., & Krooss, B. M. (2010). The Significance of Caprock Sealing Integrity for CO2 Storage. SPE International Conference on CO2 Capture, Storage, and Utilization, SPE-139588-MS. https://doi.org/10.2118/139588-MS

Cappa, F., Guglielmi, Y., Nussbaum, C., De Barros, L., & Birkholzer, J. (2022). Fluid migration in low-permeability faults driven by decoupling of fault slip and opening. Nature Geoscience, 15(9), 747–751. https://doi.org/10.1038/s41561-022-00993-4

Chadwick, A., & Eiken, O. (2013). Chapter 10: Offshore CO2 Storage: Sleipner natural gas field beneath the North Sea.

Chadwick, R. A., Zweigel, P., Gregersen, U., Kirby, G. A., Holloway, S., & Johannessen, P. N. (2004). Geological reservoir characterization of a CO2 storage site: The Utsira Sand,

Sleipner, northern North Sea. Energy, 29(9–10), 1371–1381. https://doi.org/10.1016/j.energy.2004.03.071

Cheng, Y., Liu, W., Xu, T., Zhang, Y., Zhang, X., Xing, Y., Feng, B., & Xia, Y. (2023). Seismicity induced by geological CO2 storage: A review. Earth-Science Reviews, 239, 104369. https://doi.org/10.1016/j.earscirev.2023.104369

Craddock, W. H., Drake, R. M., Mars, J. C., Merrill, M. D., Warwick, P. D., Gosai, M. A., Freeman, P. A., Cahan, S. M., DeVera, C. A., Lohr, C. D., Warwick, E. P. D., & Corum, M. D. (2012). Geologic Framework for the National Assessment of Carbon Dioxide Storage Resources─Powder River Basin, Wyoming, Montana, South Dakota, and Nebraska.

Dvory, N. Z., Yang, Y., & Dunham, E. M. (2022). Models of Injection-Induced Aseismic Slip on Height-Bounded Faults in the Delaware Basin Constrain Fault-Zone Pore Pressure Changes and Permeability. Geophysical Research Letters, 49(11), e2021GL097330. https://doi.org/10.1029/2021GL097330

EPA. (2024). U.S. EPA Facility Level Information on GreenHouse gases Tool (FLIGHT) [Dataset]. http://ghgdata.epa.gov/ghgp/main.do

Foote, R., Massingill, L., Wells, R., Dolton, G., & Ball, M. (1992). Geologic Framework for Petroleum Assessment of the Western Gulf Basin, Province 112 (Open-File Report) [Open-File Report]. DEPARTMENT OF THE INTERIOR U.S. GEOLOGICAL SURVEY.

Furre, A.-K., Eiken, O., Alnes, H., Vevatne, J. N., & Kiær, A. F. (2017). 20 Years of Monitoring CO2-injection at Sleipner. Energy Procedia, 114, 3916–3926. https://doi.org/10.1016/j.egypro.2017.03.1523

Galloway, W. E. (2008). Chapter 15 Depositional Evolution of the Gulf of Mexico Sedimentary Basin. In Sedimentary Basins of the World (Vol. 5, pp. 505–549). Elsevier. https://doi.org/10.1016/S1874-5997(08)00015-4

Gao, X., Yang, S., Shen, B., Tian, L., Li, S., Zhang, X., & Wang, J. (2023). Influence of Reservoir Spatial Heterogeneity on a Multicoupling Process of CO2 Geological Storage. Energy & Fuels, 37(19), 14991–15005. https://doi.org/10.1021/acs.energyfuels.3c02784

Godec, M. L., Kuuskraa, V. A., & Dipietro, P. (2013). Opportunities for Using Anthropogenic CO_2 for Enhanced Oil Recovery and CO_2 Storage. Energy & Fuels, 27(8), 4183–4189. https://doi.org/10.1021/ef302040u

Jung, Y., Pau, G. S. H., Finsterle, S., & Pollyea, R. M. (2017). TOUGH3: A new efficient version of the TOUGH suite of multiphase flow and transport simulators. Computers & Geosciences, 108, 2–7. https://doi.org/10.1016/j.cageo.2016.09.009

Kaldi, J., Daniel, R., Tenthorey, E., Michael, K., Schacht, U., Nicol, A., Underchultz, J., & Backe, G. (2011). Caprock Systems for CO_2 Geological Storage. IEA Greenhouse Gas R&D. Programme (IEAGHG). https://ieaghg.org/publications/caprock-systems-for-co2-geological-storage/

Kaldi, J., Daniel, R., Tenthorey, E., Michael, K., Schacht, U., Nicol, A., Underschultz, J., & Backe, G. (2013). Containment of CO2 in CCS: Role of Caprocks and Faults. Energy Procedia, 37, 5403–5410. https://doi.org/10.1016/j.egypro.2013.06.458

Koehn, L., Phillip, P. S., Godbey, W., Verne, M., Fowler, N., McCrady, P., & Pollyea, R. M. (2023). First-order CO2 trapping characteristics of fold-and-thrust belts: Assessing carbon storage potential in the Appalachian Basin and beyond. The Leading Edge. https://doi.org/10.1190/tle42110755.1

Koehn, L., Romans, B. W., & Pollyea, R. M. (2023). Assessing reservoir performance for geologic carbon sequestration in offshore saline reservoirs. Energy Advances, 2(12), 2069–2084. https://doi.org/10.1039/D3YA00317E

Korbøl, R., & Kaddour, A. (1995). Sleipner vest CO2 disposal—Injection of removed CO2 into the utsira formation. Energy Conversion and Management, 36(6–9), 509–512. https://doi.org/10.1016/0196-8904(95)00055-I

Luo, J., Xie, Y., Hou, M. Z., Xiong, Y., Wu, X., Lüddeke, C. T., & Huang, L. (2023). Advances in subsea carbon dioxide utilization and storage. Energy Reviews, 2(1), 100016. https://doi.org/10.1016/j.enrev.2023.100016

Ma, J., Li, L., Wang, H., Du, Y., Ma, J., Zhang, X., & Wang, Z. (2022). Carbon Capture and Storage: History and the Road Ahead. Engineering, 14, 33–43. https://doi.org/10.1016/j.eng.2021.11.024

Mazzoldi, A., Hill, T., & Colls, J. J. (2011). Assessing the risk for CO2 transportation within CCS projects, CFD modelling. International Journal of Greenhouse Gas Control, 5(4), 816–825. https://doi.org/10.1016/j.ijggc.2011.01.001

Meckel, T. A., Bump, A. P., Hovorka, S. D., & Trevino, R. H. (2021). Carbon capture, utilization, and storage hub development on the Gulf Coast. Greenhouse Gases: Science and Technology, 11(4), 619–632. https://doi.org/10.1002/ghg.2082

National Energy Technology Laboratory. (2015, September). Carbon Storage Atlas. National Energy Technology Laboratory.

National Energy Technology Laboratory. (2020, April 13). Safe Geologic Storage of Captured Carbon Dioxide – DOE's Carbon Storage R&D Program: Two Decades in Review. National Energy Technology Laboratory.

https://netl.doe.gov/sites/default/files/Safe%20Geologic%20Storage%20of%20Captured%20Carbon%20Dioxide_April%2015%202020_FINAL.pdf

Orivri, U. D., Chanda, P., Johnson, L., Koehn, L. W., & Pollyea, R. M. (2025). Opportunities and challenges for geologic CO2 sequestration in carbonate reservoirs: A review. International Journal of Greenhouse Gas Control. https://doi.org/DOI:10.1016/j.ijggc.2025.104342

Paluszny, A., Graham, C. C., Daniels, K. A., Tsaparli, V., Xenias, D., Salimzadeh, S., Whitmarsh, L., Harrington, J. F., & Zimmerman, R. W. (2020). Caprock integrity and public perception studies of carbon storage in depleted hydrocarbon reservoirs. International Journal of Greenhouse Gas Control, 98, 103057. https://doi.org/10.1016/j.ijggc.2020.103057

Pollyea, R. M., Fairley, J. P., Podgorney, R. K., & Mcling, T. L. (2014). Physical constraints on geologic CO2 sequestration in low-volume basalt formations. Geological Society of America Bulletin, 126(3–4), 344–351. https://doi.org/10.1130/B30874.1

Robertson, E. (1988). Rock Thermal Properties (Open-File Report) [Open-File Report]. UNITED STATES DEPARTMENT OF THE INTERIOR GEOLOGICAL SURVEY.

RockWare. (2024). PetraSim User Manual. RockWare. https://www.rockware.com/downloads/documentation/petrasim/PetraSimManual.pdf

Rosen, G., Raddatz-Bopp, A., Rodosta, T., & Aljoe, W. (2024). Carbon Storage Assurance Facility Enterprise (CarbonSAFE): Carbon Storage Infrastructure Development for a Sustainable Future.

Sachde, D., Dombrowski, K., Davis, D., McKaskle, R., & Lundeen, J. (2022). Offshore Oil and Gas Infrastructure Reuse for CCS: Opportunities and Challenges in the U.S. Gulf of Mexico. SSRN Electronic Journal. https://doi.org/10.2139/ssrn.4285894

Schrag, D. P. (2009). Storage of Carbon Dioxide in Offshore Sediments. Science, 325(5948), 1658–1659. https://doi.org/10.1126/science.1175750

Singh, A. P., Kant, R., Maurya, S. P., Kumar, B., Verma, N., Singh, R., Singh, K. H., Srivastava, M. K., & Hema, G. (2025). CO2 characterization using seismic inversion based on global optimization techniques for enhanced reservoir understanding: A comparative study. Acta Geophysica. https://doi.org/10.1007/s11600-025-01529-1

Smith, E., Morris, J., Kheshgi, H., Teletzke, G., Herzog, H., & Paltsev, S. (2021). The cost of CO2 transport and storage in global integrated assessment modeling. International Journal of Greenhouse Gas Control, 109, 103367. https://doi.org/10.1016/j.ijggc.2021.103367

Sohal, M. A., Le Gallo, Y., Audigane, P., De Dios, J. C., & Rigby, S. P. (2021). Effect of geological heterogeneities on reservoir storage capacity and migration of CO2 plume in a deep saline fractured carbonate aquifer. International Journal of Greenhouse Gas Control, 108, 103306. https://doi.org/10.1016/j.ijggc.2021.103306

Solomon, S. (2007). Carbon Dioxide Storage: Geological Security and Environmental Issues – Case Study on the Sleipner Gas field in Norway.

Song, Y., Jun, S., Na, Y., Kim, K., Jang, Y., & Wang, J. (2023). Geomechanical challenges during geological CO2 storage: A review. Chemical Engineering Journal, 456, 140968. https://doi.org/10.1016/j.cej.2022.140968

Sullivan, M., Rodosta, T., Mahajan, K., & Damiani, D. (2020). An overview of the Department of Energy's CarbonSAFE Initiative: Moving CCUS toward commercialization. AIChE Journal, 66(4), e16855. https://doi.org/10.1002/aic.16855

Texas Commission on Environmental Quality (TECQ). (2024, March 1). CLIMATE POLLUTION REDUCTION GRANTS PRIORITY ACTION PLAN FOR THE STATE OF TEXAS.

Tors, M., Frost, T. K., Hofstad, K. H., & Andrews, J. S. (2024). Evaluating Legacy Well Leakage Risk in CO2 Storage.

Trevino, R. H., & Rhatigan, J.-L. T. (2017). Regional Geology of the Gulf of Mexico and the Miocene Section of the texas Near-Offshore Waters. In Geological CO2 Sequestration Atlas of Miocene Strata, Offshore Texas State Waters. Bureau of Economic Geology. doi.org/10.23867/10283D

Vilarrasa, V., Carrera, J., Olivella, S., Rutqvist, J., & Laloui, L. (2019). Induced seismicity in geologic carbon storage. Tectonic plate interactions, magma genesis, and lithosphere deformation at all scales/Seismics, seismology, paleoseismology, geoelectrics, and electromagnetics/Seismology. https://doi.org/10.5194/se-2018-129

Wallace, K. J., Meckel, T. A., Carr, D. L., Treviño, R. H., & Yang, C. (2014). Regional CO_2 sequestration capacity assessment for the coastal and offshore Texas Miocene interval. Greenhouse Gases: Science and Technology, 4(1), 53–65. https://doi.org/10.1002/ghg.1380

Witrock, R. (2017). Biostratigraphic Chart of the Gulf of Mexico Offshore Region, Jurassic to Quaternary. U. S. Department of the Interior, Bureau of Ocean Energy Management.

Yang, C., Treviño, R. H., Zhang, T., Romanak, K. D., Wallace, K., Lu, J., Mickler, P. J., & Hovorka, S. D. (2014). Regional Assessment of CO_2 –Solubility Trapping Potential: A Case Study of the Coastal and Offshore Texas Miocene Interval. Environmental Science & Technology, 48(14), 8275–8282. https://doi.org/10.1021/es502152y